AN ABSTRACT OF THE THESIS OF

Erica D. Kemp for the degree of Master of Science in Water Resources Engineering presented on June 1, 2015.

Title: Sediment Transport Prototypes: Novel Methods to Disconnect Forest Roads from Streams.

Abstract approved: ____

Ben A. Leshchinsky

Unpaved roads are a critical form of infrastructure in forested landscapes but also a potential source of fine sediment that can degrade sensitive ecosystems nearby. Improved management of aggregate road surfacing can reduce sediment generation, lengthen its useful life span, reduce maintenance costs, and more importantly, mitigate the impacts of road sediment on hydrologically connected ecosystems.

This study investigated three road construction treatments and evaluated their performance based on runoff water quality, aggregate load distribution, and practicality of widespread application. Treatments included an aggregate-only control (no treatment), a biomass waddle-type filtration bale, and a geotextile-wrapped filter sand berm with a geogrid underlay. Two different aggregate varieties were used totaling six road treatment sections.

The biomass filtration bale provided no discernable filtration benefit from road aggregate sourced runoff. The geotextile-wrapped sand filtration berm produced variable results in the field, but follow-up laboratory testing indicated a substantial reduction in effluent turbidity. The geogrid reinforcement effectively reduced subgrade stress and increased aggregate bearing capacity.

Testing took place on a reconstructed unpaved forest road test track in Dunn Research Forest, Oregon, USA. A worst-case sediment scenario was produced with simulated rainfall and heavy truck traffic to mimic wet-weather timber hauling. Ditch

runoff was collected to determine filtration effect of each road treatment and surface aggregates were testing for degradation through time to determine rate of sediment generation. Field testing was performed during June and July, 2015. Data analysis is ongoing and preliminary findings are presented herein.

Hydrologic relationships and aggregate degradation rates are consistent with contemporary research. These agreements provide a metric for validating the highly-controlled experimental design. Investigators are currently developing recommendations for new best management practices employing the use of geotextile materials in unpaved forest road construction as a means of improving water quality of runoff, and aggregate performance.

Sediment Transport Prototypes: Novel Methods to Disconnect Forest Roads from Streams

by
Erica D. Kemp

A THESIS

submitted to

Oregon State University

in partial fulfillment of
the requirements for the
degree of

Master of Science

Presented June 1, 2015
Commencement June 2015

Master of Science thesis of Erica D. Kemp presented on June 1, 2015.

APPROVED:

Major Professor, representing Water Resources Engineering

Director of the Water Resources Graduate Program

Dean of the Graduate School

I understand that my thesis will become part of the permanent collection of Oregon State University libraries. My signature below authorizes release of my thesis to any reader upon request.

Erica D. Kemp, Author

ACKNOWLEDGEMENTS

I wish to express my sincere appreciation for all those who devoted their time, talent, and hard work to making this research a success. The list is long and I am sure to have left names out but every person on this list was instrumental to both the project, and my graduate experience.

Ben Leshchinsky
Kevin Boston
Arne Skaugset
Mary Santelmann
Marvin Pyles
Devlin Montefort
Alex Irving and the ASL crew
Jim Kemp
Sheralyn Kemp
Paul Weitzman
Abigail Thorpe
Robin Wortman
Jordan Vesper
Alec Martin
Chris Hale
Hunter Guogen
OSU College Forests
Mid Pacific Enterprises and construction crew

And to all the support staff in the Water Resources Graduate Program and the College of Forestry Department of Forest Engineering, Resources, and Management. Finally a special thanks to the friends I made along the way both in the WRGP and CoF, your understanding and support made the whole experience not just possible, but enjoyable.

TABLE OF CONTENTS

Page

TABLE OF CONTENTS (Continued)

Page

LIST OF FIGURES

TABLE OF FIGURES (Continued)

Figure Page

TABLE OF FIGURES (Continued)

Figure | Page

LIST OF TABLES

LIST OF APPENDICES

INTRODUCTION

Unpaved roads are the infrastructure of choice for access to managed forested lands. Their low cost, ease and speed of construction, and ability to withstand repeated heavy traffic benefit multiple industries. Despite their practical utility, forest roads are a potential source of ecological disturbance. Over time, unpaved road systems generate sediment which can collect in runoff and deposit in nearby aquatic ecosystems. For small order streams, this amounts to a substantial increase in the turbidity and suspended solids concentration (SSC) of the stream—conditions that degrade sensitive habitats such as spawning grounds for threatened salmonid species (Lane and Sheridan 2002, Madej 2004). In the Pacific Northwest region of the United States, land managers must weigh these deleterious effects of sediment transport with the practical benefit of unpaved forest roads as a means of accessing and working in forested landscapes.

New construction methods and management practices aim to combat the harmful effects of fine sediments produced in prevalent unpaved road networks within forested lands. Specifically, novel methods of filtration and retention have the potential to sequester fine sediments from an unpaved road aggregate structure. This research investigated the mechanisms of sediment generation and the use of geosynthetic materials to sequester sediment within an unpaved road system.

Three road treatment methods were tested on six road segments. One segment consists of aggregate material only, serving as a control. A second segment uses a Douglas fir (*Pseudotsuga menziesii*) biomass filtration bale. The third segment is underlain with geogrid reinforcement and uses a sand filtration berm wrapped in a geotextile. Two different aggregate varieties were used totaling six different road segments. Pressure cells located at the aggregate-subgrade interface and physical measurements of road performance were placed to provide insight into the physics of aggregate degradation. Simulated rainfall and truck traffic produced a worst-case scenario sediment event in which runoff collected from each road treatment could be analyzed for turbidity and SSC to determine treatment efficacy (Sheridan, et al. 2006, Toman and Skaugset 2011). A cost-benefit analysis of each treatment will then be used to inform best practices recommendations based on study results.

Investigators expected to find a sequestration benefit in road segments using either of the two treatment methods. The sand filtration berm was expected to provide greater sediment sequestration than the biomass filtration berm. Sequestration benefit was expected to exist for both aggregate sources. Aggregate degradation and subsequent sediment generation was expected to be a function of cyclic loading from truck traffic (Lekarp, Isacsson and Dawson 2000). The geogrid reinforcement present at the aggregate-subgrade interface in two of the road segments was expected to improve the mechanical performance of the aggregate (Leshchinsky and Ling 2013b) and reduce the amount of sediment generated in those segments. Given the growing popularity of geosynthetic materials in numerous road construction applications, investigators intend to provide best practice recommendations using these materials that will keep construction costs low while providing the practical benefit of sediment sequestration in unpaved forest roads.

Background

Sediment generation occurs naturally, and sediment migrates via multiple natural processes. Wind, surface erosion, soil creep, rivers, streams, and even the ocean are all vectors of sediment transport. Innate sediment production and transport in forest environments poses difficulties for researchers in identifying where sediment originates. Locating the source and cause of sediment production, either from natural processes or anthropogenic influence, determines appropriate mitigation strategies.

In the forests of the Pacific Northwest, sediment produced from anthropogenic activities often originates in logging roads or in disturbed terrain (Megahan and Kidd 1972, Beschta 1978, Reid and Dunne 1984). This may include loosely compacted bare soil from skid trails or other logging activities, excavation sites, and road cut and fill slopes in addition to roads themselves (Bilby, Sullivan and Duncan 1989, Lane and Sheridan 2002). Many logging roads are built on ridgelines, away from bodies of water. This hydraulically disconnects unpaved roads from streams and other aquatic habitat.

Ridgeline roads are located far enough away from streams such that sediment carried away from the road via runoff settles out over rough terrain before reaching a stream. Riparian buffers serve the same purpose for roads that must be constructed stream-adjacent but factors such as buffer width and site hydrology control the effectiveness of the buffer (Castelle, Johnson and Conolly 1994). For road segments that must cross a stream or other body of water, there is little in the way to hydraulically disconnect the road from these aquatic areas. Due to the impracticality of building paved road networks in remote forested regions and the inevitability of stream-adjacent road networks, land managers and policy makers need best management practices (BMPs) to address this long-standing challenge.

The contemporary spotlight on upper reach stream habitat for threatened salmonid species has initiated efforts to minimize the impacts of unpaved forest roads. Past investigations revealed that use of high-quality aggregate, minimal truck traffic, and infrequent rainfall are all factors that reduce sediment transport from forest roads. Unfortunately, forest roads are often built with locally-sourced aggregate—for economic reasons—of poor quality and the roads are built only where required thus high traffic volumes are common (Foltz and Truebe 2003). Compounding these negative influences is the stochastic nature of rainfall-runoff events. Solutions to mitigate sediment transport in forest roads must account for low-quality aggregate sources, high traffic volumes, and hydrologic site characteristics. One approach to addressing the sediment generation from aggregate surfacing involves the use of innovative methods for retaining the sediment that is inevitably generated within the road prism. This study will focus specifically on the surface aggregate of an unpaved road system, and the sediment generated from that aggregate.

Research Objectives

The objectives of this investigation are:

- To quantify the amount of sediment generated within an unpaved forest road as a function of truck traffic.

- To quantify the amount of sediment transported away from an unpaved forest road when implementing sediment sequestration treatments during a wet-weather hauling scenario.
- To evaluate the efficacy of sediment sequestration treatments and their viability in commercial applications.

LITERATURE REVIEW

Forest Roads and Water Quality

The timber industry has long been under scrutiny for unfavorable environmental impacts. Logging activities do increase sediment yield, but the associated construction of unpaved roads produces sediment loads orders of magnitude larger than logging itself (Megahan and Kidd 1972). The exact source of these sediment loads and their vectors of transport are the subject of a decades-long search for practical environmental solutions. Many studies have tried to predict and measure the effects of unpaved forest roads on adjacent aquatic habitat (Lane and Sheridan 2002, Toman and Skaugset 2011). Most of these investigations have found that the construction and presence of unpaved roads and associated earthwork is a principal source of fine sediments that are carried through runoff to nearby streams (Megahan and Kidd 1972, Johnson and Beschta 1980, Reid and Dunne 1984, Lane and Sheridan 2002). But despite exhaustive efforts, investigators still find conflicting results in identifying the dominant drivers of sediment production; this obfuscates the prediction of sediment loads to streams (Luce and Black 1999, Lane and Sheridan 2002, Toman and Skaugset 2011). Compiling knowledge obtained through past research and identifying gaps of information will help direct future progress on the issue of forest road sediment.

Prediction of Sediment Generation

Multiple factors affect the generation and yield of sediment on unpaved forest roads. The ability to predict sites which are highly susceptible to large sediment yields would allow land managers to focus environmental mitigation efforts. Material tests, site hydrology, and surface models all provide predictions of sediment yield, but their application and effectiveness is not universal.

Surface erosion models are a popular tool for predicting annual sediment load from unpaved road segments. Skaugset et al. (2011) compared the measurement of annual sediment yield with four common sediment prediction models, each of which overestimated the sediment production of 44 road segments by at least 100 percent. The investigators point out that the climate in the Pacific Northwest is generally not conducive to surface erosion and therefore existing models (most developed for agriculture) are poorly suited for use in this region (Skaugset, et al. 2011). Even in forested environments outside the United States, researchers have found the use of surface erosion models to be inappropriate and ineffective for aggregate roads in densely vegetated regions (Sheridan, et al. 2006). Models that are not based on surface erosion may prove more effective for predicting sediment yield, but the development of these models requires the knowledge of which parameters have the greatest influence over sediment generation in forest roads.

Efforts to predict sediment generation in aggregate have focused on either large, watershed scale sediment budgets, or small, confined laboratory test configurations (Beschta 1978, Reid and Dunne 1984, Bilby, Sullivan and Duncan 1989, Luce and Black 1999, Foltz and Truebe 2003, Toman and Skaugset 2011). In a controlled analysis of aggregate performance, Foltz and Truebe (2003) found that aggregate gradation was a strong predictor of both runoff volume and sedimentation. Their study gathered aggregate samples from four northwestern states and tested them in a small, confined test track with simulated rainfall and hauling events equivalent to 200 truck passes. They found that particle size distribution, specifically percent by mass passing a 0.6-mm sieve (ASTM No. 30), was a strong indicator of sedimentation in an unpaved road under wet weather log truck hauling conditions. Given a constant rainfall rate, they recommended minimizing the amount of fine material passing a 0.6-mm sieve (ASTM No. 30) while maintaining at least 12 percent by mass as a beneficial minimum for road stability (Foltz and Truebe 2003).

Results from Toman and Skaugset (2011) were consistent with findings from Foltz and Truebe (2003). Toman and Skaugset conducted large scale tests of different types of aggregate and road construction in partnership with private land owners across the Northwest. Segments of existing logging roads were reconstructed with different design treatments and observed under wet-weather hauling. Sediment transported via runoff was collected from flumes in roadside ditches and truck tickets were gathered as a measurement of traffic loading. Each road segment included sections with and without geotextiles and geogrids, and used locally sourced aggregate surfacing. Investigators anticipated that sediment generation would be a function of subgrade-aggregate mixing and thus road sections with use of geotextiles and/or geogrids would generate less sediment.

Findings were statistically inconclusive, leading the authors to believe that sediment generation is largely a function of surface aggregate, and thus best predicted by percent passing a 0.6-mm (ASTM No. 30) sieve. Specifically, they found that aggregate materials with 14% or greater concentration of mass passing a 0.6 mm sieve (ASTM No. 30) were connected to road segments that produced larger volumes of sediment (Toman and Skaugset 2011). This is consistent with the 12% ideal mass concentration passing a 0.6 mm sieve found by Foltz and Truebe (2003).

Hydrologic Relationships

Prior research investigations found a distinct relationship between turbidity, total suspended solids (TSS) and rainfall intensity (Langbein and Schumm 1958, Lane and Sheridan 2002, Miller 2014). Although TSS are a function of stream energy, it correlates with turbidity because finer particles remain in suspension under stagnant conditions. Therefore, increased sediment bedload to a stream will result in increased TSS and increased turbidity. The linear relationship between these two parameters allows researchers to collect discrete samples which simplifies data collection and interpretation. More importantly, these parameters function as a means of assessing water quality to determine the environmental impact of forest roads on aquatic systems (Lane and Sheridan 2002).

Proportional to rainfall, runoff is also directly related to sediment yield. Without runoff, turbid waters and suspended sediments could not reach rivers and streams. Foltz and Truebe (2003) verified this and demonstrated that the amount of sedimentation from aggregate was directly proportional to the volume of runoff exiting their test track under simulated rainfall conditions.

Miller and Skaugset (2014) set up flumes and weirs to measure the runoff from segments of logging roads in the Oregon Coast Range. ISCO pump samplers were programmed to sample ditch runoff when rainfall and turbidity increased beyond a threshold value. This sampling design produced high temporal resolution time series of both runoff volume and sediment. These data agree with Lane and Sheridan (2002) and Foltz and Truebe (2003) that the strongest predictor of sediment volume within the runoff was rainfall itself (Miller 2014). Other factors including truck hauling, road material, and ditch hydrology had less influence on sediment yield (Miller 2014). This finding encourages further research under controlled rainfall conditions in order to determine the anthropogenic influences of sedimentation in aggregate roads.

Influence of Truck Traffic

Truck traffic is a known mechanism of aggregate degradation. The rate of degradation is linked to number and magnitude of loads (Lekarp, Isacsson and Dawson 2000, Sheridan, et al. 2006). Degradation and abrasion of road materials produces fine sediments, while also dislodging existing fines, often used in aggregate surfacing for traction and aggregate bonding. Although aggregate quality and strength play an important role in the rate and amount of degradation, Foltz and Truebe (2003) found relationships between rutting, runoff volume, and sediment production. Among different rock types, steady simulated rainfall, and repeated loading, they observed an increase in sediment production with both the presence and length of rutting (Foltz and Truebe 2003). Although their investigation inspected test tracks which experienced only 200 truck passes, Foltz and Truebe (2003) were able to determine that the combined influence of truck traffic and aggregate quality created a statistically significant difference in sediment production. Insight into the effect of sediment production and degradation as a function of truck traffic may further inform this relationship.

Reaching similar conclusions, Toman and Skaugset (2011) noted that among their three test sites, all using different aggregates, the roads that exhibited rutting were larger producers of sediment in runoff. Their study was not designed specifically to investigate rutting, and therefore they were unable to provide more conclusive results. Others, however, have linked aggregate strength to rutting (Giroud and Han 2004).

Giroud and Han (2004) developed design criteria for use of geogrid reinforcement on base course material within an unpaved road. Their method calibrates factors to fit parameters in several design case studies. Notably, they link heavy truck traffic, number of loads, and subgrade beating capacity to road rutting (Giroud and Han 2004). Their method illustrates how the use of geogrid reinforcement reduces the required thickness of a base course material given a maximum rutting depth criteria (Giroud and Han 2004). These findings should also hold true for aggregate surface material of similar properties.

Role of Aggregate Strength and Material Properties

Rutting is one of many factors that illustrate the rate and magnitude at which aggregates experience permanent strain deformation. Lekarp, Isaacson, and Dawson (2000) found that stress magnitude and direction, number of loads, degree of saturation, load history, compaction, gradation size and distribution, and aggregate material were all parameters that influence the complex response to strain in unbound aggregates.

Although sieve analysis has been shown to be a good predictor of sediment generation in aggregate road material, the material properties of aggregates also influence susceptibility to abrasion and erosion (Foltz and Truebe 2003). Foltz and Truebe (2003) found that the “sand equivalent test and the PM20 portion of the Oregon air degradation test” best predicted aggregate quality, in this case, resistance to erosion and abrasion. These two tests were the most statistically significant indicators among the seven test procedures in the study using both ANOVA and correlation coefficients as metrics (Foltz and Truebe 2003).

Aggregate strength improves resistance to degradation but also reveals other performance considerations. Leshchinsky and Ling (2013a, 2013b) found that on a study of railroad ballast, aggregate strength was tied to performance and longevity, as well as an ability to distribute loading to supporting subgrade materials. The same should hold true for forest roads, where the occurrence of rutting from repeated truck traffic can be minimized by the use of stronger aggregates to minimize subgrade stresses (Toman and Skaugset 2011).

Use of Geosynthetics

Leshchinsky and Ling (2013b) also studied the effects of geosynthetics on aggregate strength. They found a positive correlation between increased confinement and improved aggregate strength and performance. Confinement with the use of geocells immobilized aggregate from deformation under loading, and prevented abrasion and fracture when confined (Leshchinsky and Ling 2013b). Geogrids function in a similar mechanism, preventing movement and enabling confinement through granular interlock when aggregate grains are adequately sized and angular.

Other forms of geosynthetic materials provide different benefits. Geotextiles have long been used as a means of filtration (Wu, et al. 2006). Non-woven geotextiles, often known as “filter fabrics” provide marginal tensile strength in comparison to geogrids or geocells, but allow water to permeate the fabric while retaining grains of a specified size (Wu, et al. 2006). These membranes are chosen for filtration applications based on mean opening size—a property that can be connected to problematic sediment concentrations. While there are no solutions to entirely prevent sediment generation in an in-use, unpaved forest road, geosynthetic filtration promises a means to sequester the sediment and prevent it from leaving the road network.

Next Steps

Extensive research conducted in the past has not provided accurate tools to predict sediment generation from unpaved forest roads (Sheridan, et al. 2006, Skaugset, et al. 2011). External predictors of sediment generation such as truck traffic and rainfall-runoff relationships have been established and measurement of sediment through turbidity and TSS has provided an effective way to measure the influence of unpaved roads on water quality. These relationships form an important foundation in understanding the origins and movement of sediment. Moving forward, research must be focused on specific and isolated processes that exacerbate sediment generation within the road prism and how these can be minimized. When those measures are exhausted, the remaining sediment with potential to escape an unpaved road must be sequestered. A tandem cause-effect approach will provide necessary information required to tackle this problem.

Isolating specific mechanisms of sediment production and retention requires isolation and observation of known variables. An ideal study design would mimic the natural circumstances of wet-weather truck hauling in forest roads without sacrificing the experimental control that allows for precise parameter observation. This experiment aims to fill in the gaps between large scale road studies and small scale laboratory work.

METHODS AND MATERIALS

Conceptual Framework

In order to quantify relationships between multiple parameters, this study uses a small, isolated, field-scale experiment to increase parameter control and reduce response variability. Relationships between sediment transport, truck traffic, aggregate degradation, and subgrade pressure will be quantified. This requires control of other system variables including sediment source area, load cycles, and rainfall rate. Testing in a field environment will allow investigators to determine if road treatments are practical for large-scale application on unpaved forest road networks.

Experimental Methods

Site Description

A test track was constructed on an existing road in Dunn Forest, Oregon, USA. The site is located in the eastern foothills of the central Oregon Coast Range in a mixed stand of predominantly Douglas fir (*Pseudotsuga menziesii*) and Grand fir (*Abies grandis*) (McDonald-Dunn Forest Plan 2005). Located in a transitional zone between the Coast Range and the Willamette Valley, the area experiences mild wet winters and warm dry summers (McDonald-Dunn Forest Plan 2005). Native subgrade soils at the site belong to the Price-MacDunn-Ritner complex. Soils consist of silty clays which are well-drained with “moderately high” permeability (NRCS 2009). The test site, located on the 320 road in Dunn Forest, drains into the Soap Creek watershed in the Willamette River basin. (See Appendix A for Dunn Forest road map.)

The test track was designed in order to collect road runoff and examine aggregate degradation of six different test sections under simulated, wet-weather loading conditions. Each section was confined to a control volume (consistent sediment source area across all test sections) and segregated from the subgrade in order to isolate and study the sediment produced from the surface aggregate. Therefore, rainfall was simulated over the road surface using a sprinkler system with a fixed intensity to eliminate runoff contamination from the hillslope. Testing took place over a dry, two-day period from June 30 to July 1, 2014.

Construction

The selected test track was a 36.6 meter (120 feet) section of road with a 4% grade. Each test section within the track was 3.6 meters (12 feet) in width by 6.1 meters (20 feet) in length with a continuous ditch on the inboard side of the road. Construction of the test site took place in a two-day period from June 26 through 27, 2014. The roadway was prepared by first excavating the existing surface aggregate to a depth of approximately 30 cm (12 inches) to ensure a subgrade of native material. Spoils were hauled off-site and the native base material was graded at approximately 3-4% in-slope. A Clegg impact hammer was used to find Clegg impact values (CIV) of the native soil as a reliable in-situ measure of subgrade hardness (Clegg 1980). A vane shear was used to determine undrained shear strength of the soil and soil core samples were collected to calculate subgrade water content prior to testing. Subgrade properties are summarized in Table 1. Field data measurements can be found in Appendix B.

Property	Site Minimum	Site Maximum	Site Average
Clegg impact value	4.1	9.0	6.3
Undrained shear strength (kPa)	135	260	189
Water content	0.25	0.42	0.34

Table 1: Summary of Clegg impact values, undrained shear strength, and water content of road subgrade material at testing site.

Prior to backfill, pressure cells (Tokyo Sokki Kenkyujo KDE-500 Pressure cells, 50 Hz measurement frequency) were placed within the subgrade/aggregate interface underneath the centerline of the inside tread of the wheel line. Data from pressure cells were collected at a frequency of 50 Hz using two Campbell Scientific CR31000 Data Loggers.

Upon completion of in-situ testing and subgrade preparation, a layer of biaxial geogrid (Alliance Geo BX2020) was placed beneath the inner two test sections as a treatment means of ground improvement (Figure 1). Then, six runoff collection flumes were placed on top of the native soil, or geogrid, respectively. The flumes were constructed from Flexible Ethylene Propylene Diene Monomer (EPDM) liners at 2.5 mm (0.10 inches) of thickness, and mechanically connected to flexible PVC water bars to maintain vertical side-walls (Figure 1). The road was then backfilled 8-10 cm (3-4 inches) with new aggregate material. The upper three test sections received well-graded basaltic aggregate and the lower three sections contained poorly graded micaceous schist aggregate.

Figure 1: Test track construction. Geogrid placement over subgrade (left) and buried runoff collection flumes in roadway (right).

On top of the first lift of aggregate, 10 cm (4 inch) diameter woven high density polyethylene (HDPE) bags filled with aggregate, each approximately 1.2 meters (4 feet) long, were placed perpendicular to the road and in line with the pressure cells on the inside tread of the road. This served as a means of retrieving representative samples of road material during fixed testing intervals. An additional 10 cm (4 inches) of aggregate was placed on top of the aggregate separation bags until approximately 40 cm (15 inches) of aggregate had been placed on the road. Subsequently, a mechanical vibratory wheel roller compacted the surface on the final lift providing a total compacted surface of approximately 30 cm (12 inches). Refer to Figure 2 for final road configuration.

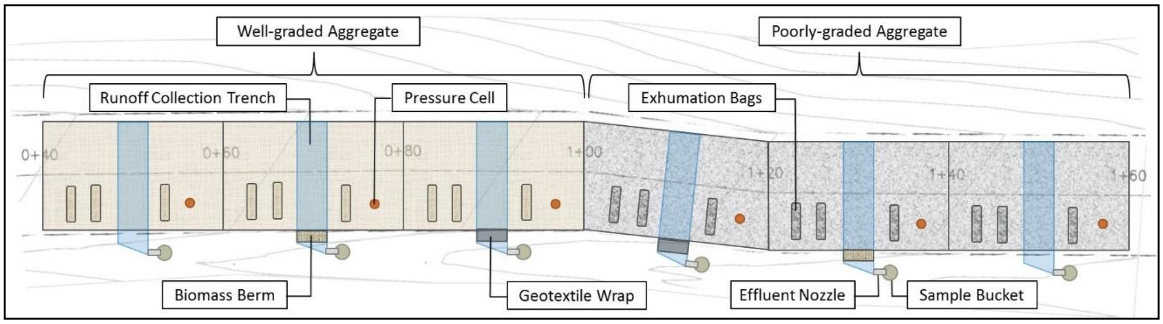

Figure 2: Dunn Forest test track configuration. Road slopes downward at 4% grade from left to right.

Treatments

Three different treatments were tested for sediment sequestration efficacy. Each treatment was constructed with two separate types of aggregate, well-graded and poorly-graded, for a total of six test sections. Utilizing more than one aggregate source provides some insurance to determine if any treatment effect is the result of the treatment itself, or the material used.

The first road treatment involved the use of a nonwoven geotextile fabric (Alliance #100 Filtration Geotextile) wrapped around filter sand (Figure 3) to create a filtration berm on the inboard side of the road. This treatment was underlain with a geogrid to avoid problems arising from a lack of interlock between aggregate surfacing and base material shown by Toman and Skaugset (2011).

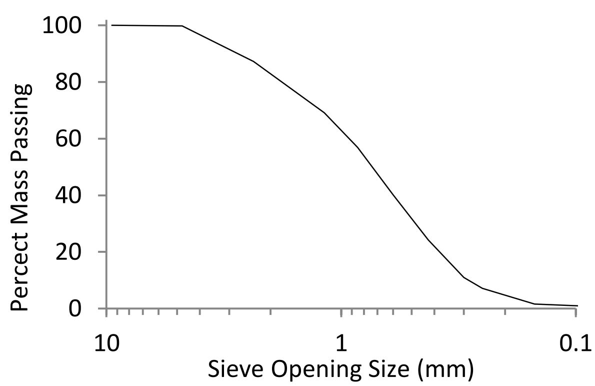

Figure 3: Stayton filter sand gradation.

The second road treatment used Douglas fir (*Pseudotsuga menziesii*) shavings packed inside porous sand bags to create a different type of berm on the inboard side of the road. Both treatments assume an ideal scenario of all runoff passing through the berms before entering the ditch where water sampling occurred.

The final treatment was a control section of road, to see how well each berm performed in comparison to untreated aggregate. See Table 2 for a treatment schedule for all six test sections and Figure 4 for cross-sections of each treatment.

Section	Abbreviation	Aggregate Variety	Filtration Treatment	Reinforcement Type
1	WGC	Well-graded	Control	None
2	WGB	Well-graded	Biomass berm	None
3	WGG	Well-graded	Geotextile / filter sand	Geogrid underlay
4	PGG	Poorly-graded	Geotextile / filter sand	Geogrid underlay
5	PGB	Poorly-graded	Biomass	None
6	PGC	Poorly-graded	Control	None

Table 2: Treatment schedule for all six road sections.

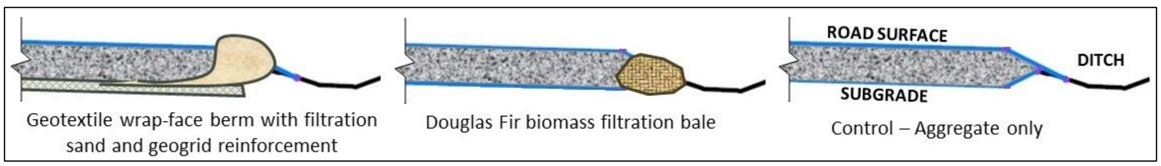

Figure 4: Road treatment cross sections.

Hydrologic Sampling

Simulated rainfall was produced using a portable sprinkler system. A series of Rainbird 3500 Series Rotor sprinkler heads were spaced evenly along the outer edge of the road such that each test section received even coverage. The sprinkler heads were connected to a 19 mm diameter rubber hose that hooked up to a water truck and water pump (E. M. Toman 2007). The system provided an average precipitation rate of 15 mm (0.6 inches) per hour, representative of a semi-annual storm event in the central Oregon Coast Range (Goard 2003). Wedge rain gauges were placed in the center of the road during testing to measure rainfall intensity and coverage during the first 300 truck passes. Runoff from the rainfall was collected in the inboard ditch for water quality testing.

Turbidity data were recorded from the road section using the EPDM flumes to channel runoff towards the road ditch. Runoff collection flumes within each test section provided a control volume from which to take runoff measurements. The simulated rainfall percolated through the surface aggregate until reaching the impermeable liner layer at the bottom of the buried flume. Water was allowed to run off the in-sloped road prism towards the ditch where it was funneled into a plastic bucket. An ISCO pump sampler took 500 mL runoff samples at approximate intervals of 25 truck passes. The buckets where road-originating effluent was collected were emptied every 25-50 truck passes to prevent enrichment of the runoff samples by concentrated suspended solids in the bucket. This sampling continued for 600 truck passes. When truck traffic was discontinued, the sprinkler system continued simulated rainfall for another 40 minutes. In this period of time, the runoff was sampled every ten minutes. The last four samples are intended to provide information on whether or not the road began a 'cleaning' cycle once vehicular traffic had ceased.

Truck Traffic

Both the pressure cells and the aggregate bags provided means by which to compare the effects of truck traffic on aggregate degradation and concentration of suspended sediment in runoff. Log truck traffic was simulated with two fully loaded, 3-axle dump trucks which had a vehicle weight of 21,300 kg (47,000 lbs), and a rear axle load of 7,700 kg (17,000 lbs). Their approximate speed was 4.5 meters per second (10 mph). One truck pass includes all three axles of the truck passing over the road in one direction. Two trucks were used to expedite load testing.

The aggregate separation bags buried within the road prism provided a means to measure degradation over time as a function of cyclic loading (truck traffic). The woven HDPE fabric of the bags provided a flexible, yet durable material to segregate known volumes of aggregate from the road that were later exhumed and analyzed for change in gradation. Three aggregate bags were placed per test section and were removed at intervals of 100, 300, and 600 total vehicle passes. Aggregate material in the bags were screened and weighed prior to construction and after exhumation to compare change in gradation by mass.

Aggregate Performance

A continuous time series of pressure data was collected for each test section and can be compared to gradation analysis, as well as sediment concentration in runoff. The pressure data, collected at 50 data points per second (50 Hz), provided a means of quantifying applied stresses within the aggregate surfacing after repetitive loading, informing mechanical performance of the road and the individual aggregate particles.

Data Analysis

Turbidity

Turbidity was measured to quantify the nature of the runoff from the test sections under wet-weather hauling conditions. Turbidity was measured using a Hach 2100P turbidimeter. Water samples from the field were kept in ISCO sample bottles and placed in a refrigerated storage room to prevent any microbial growth prior to testing. Once removed from the cooler, each sample was agitated to suspend any solids or fine materials that had settled in the bottom of each bottle. Immediately upon agitation approximately 15 mL of the sample was poured into a sample vial for turbidity testing.

The Hach 2100P is only capable of reading samples up to 1000 NTUs. The majority of road runoff was in excess of this threshold and therefore most samples had to be diluted in order to use the turbidimeter. Each dilution consisted of 5 mL of turbid water, to 10 mL of pure DI water; a 1:3 dilution ratio. Each sample was diluted until the turbidimeter provided a reading. The total turbidity for each sample was then calculated using the following formula:

$$\frac{\text{Measured NTU}}{(1/3)^{\#\text{ of Dilutions}}} = \text{Sample NTU} \tag{1}$$

It is important to note that the turbidity readouts from the Hach 2100 P deliver only three significant figures. Also notable, is that the heavier solids in each sample began to settle out immediately upon agitation. This likely caused some solids loss during each sample dilution causing the turbidimeter to underestimate the turbidity of each sample. However, given the limited precision of the turbidimeter, these discrepancies are assumed to be negligible.

Suspended Solids

Once turbidity was recorded, the remainder of each water sample was used to calculate suspended solid concentration. Each sample was poured into a metal tin and placed in an oven (either a Dispatch LEB Series or a Fischer Scientific Isotemp Oven) at 105º C (221º F) for at least 24 hours to evaporate all the water in the sample. The metal containers were weighed before the samples were added, and after each sample was dehydrated to calculate the total solid material present. Additionally, the sediment was removed from the tins and weighed again as a means of redundancy to avoid error in the calculations. Each sample was placed in its own plastic bag, labeled, and stored for subsequent permeability testing.

Each water sample was weighed in its bottle prior to being poured into the metal tins for drying (Ohaus ARC 120 scale). Once empty, the bottles were washed and dried and weighed. The weight of the water sample was recorded as the difference of these values. A standard procedure for estimating the sample volume based on the sample and solid weights is outlined in Appendix C (along with other standard laboratory procedures). The total sample volume is then used to calculate suspended solid concentration (SSC) according to Equation 2.

$$\frac{\text{weight of suspended solids (mg)}}{\text{sample volume (L)}} = \text{SSC mg/L} \tag{2}$$

Permeability and Filtration

The Stayton filter sand and non-woven geotextile wrap were used in laboratory tests to determine the sediment sequestration benefits of the geotextile wrap-faced berm treatment under idealized conditions. A sand column placed in a permeameter provided a means of measuring the permeability of the filter sand, and filtration benefits provided by the filter sand and non-woven geotextile wrap. To determine permeability of the filter sand, clean water was added to the sand column and varying head levels, then the rate of effluent production was recorded using a graduated cylinder and a timer. To determine filtration benefits provided by the filter sand and geotextile, the same set-up was used but turbid water was added to the sand column and effluent samples were measured for turbidity. Two of these trials included a flushing period after sediment loading to record the recovery time of the effluent to pre-event levels.

Effluent samples were taken at decreasing frequency during both loading (turbid influent) and flushing (clean influent) phases of each test. The reason for this was to capture the expected exponential decay behavior of turbidity in the effluent.

Aggregate Degradation

Prior to burial within the road prism, 18 HDPE aggregate separation bags were filled with either well-graded or poorly-graded aggregate that had been screened to determine their gradation using a (Gilson Screen Co. Test-Master Model No. TM-3 screening machine. Standard ASTM screen sizes were used which included 2”, 1 ½”, 1”, ½”, ⅜”, and ¼”. A Mettler PF 16 scale was used to weigh the samples passing each screen size and gradation tables were compiled (Appendix D). Upon exhumation from the road surface, the HDPE aggregate bags were emptied into buckets and air dried for several weeks at temperatures up to 35º C (95º F). Once dry, the aggregate samples were re-screened to determine change in gradation by mass (Appendix E). Table 3 shows which samples were buried in each test section and how many truck passes occurred prior to removal from the road.

Truck Passes	Section 1	Section 2	Section 3	Section 4	Section 5	Section 6
100	WG 2	WG 5	WG 8	PG 2	PG 5	PG 7
300	WG 3	WG 4	WG 7	PG 1	PG 4	PG 8
600	WG 1	WG 6	WG 9	PG 3	PG 6	PG 9

Table 3: Aggregate separation bag sample numbers by test section and number of truck passes.

Aggregate separation bags were removed with a jack hammer and pick axe. Care was taken not to disturb the woven HDPE sheathing. Despite the effort, some of the aggregate bags were torn either from abrasion in the road prism or during the removal process and small amounts of material were lost. Due to the change in sample mass the percent passing by weight was calculated as a more accurate representation of the change in gradation as a function of truck traffic. This assumes that the sample mass lost during the removal process was representative of the sample gradation.

In addition to the screen sieving for large diameter gradation, material that passed ¼" was also wet-sieved using 8-inch ASTM sieves numbers 4, 10, 40, 100, and 200 in order to determine the fines (material passing the no. 200 sieve) present in each aggregate sample. After mechanical agitation of the sieves, the sieve stack was placed under running water to wash away the fine particles that adhered to larger grain sizes. The mass of the fine material was calculated as the difference between the total mass passing the ¼" screen and the total mass of grain sizes retained above the no. 200 sieve. Because wet-sieving is a destructive process, only post-test gradation curves include particle sizes less than ¼".

Subgrade Stress

Data from the pressure cells were recorded in data loggers and downloaded electronically. Once these files were downloaded they were converted into both spreadsheet format and comma delimited text files for analysis. Using the statistical program R, a code was created to help remove excess data points that were recorded while no traffic was present on the road (Appendix F). The reduced data points were compiled to create six time series of strain data. The maximum pressure of each truck pass was determined and extracted to observe the change in strain as a function of total truck passes for each test section (See Appendix G for max pressures table).

Expected Outcomes

The intended outcome of this study is to quantify the relationship between truck traffic and sediment production, and the benefit of each treatment regime. Specifically, the study seeks to determine whether:

- Aggregate degradation is a function of cyclic loading (truck passes) and a source of fine sediments in the pavement surface layer;

- Runoff transports surface-layer sediment away from the road prism. Runoff is expected to be dominated by subsurface flow;
- The biomass berm and geotextile wrap will both provide a sediment sequestration benefit that can be quantified.

Scope of Inference

Related research developed relationships between performance of various aggregates (Foltz and Truebe 2003), degradation as a function of cyclic loading (Lekarp, Isacsson and Dawson 2000, Leshchinsky and Ling 2013b), and turbid runoff as a function of rainfall rate (Langbein and Schumm 1958, Lane and Sheridan 2002). Using sediment removal techniques, it is expected that study results can be extrapolated for a range of conditions. Factors known to limit the scope of inference include specific road prism geometry, limited temporal scale of observation, and small sample sizes. These limitations confines the applicability of this investigation to quantitative descriptions of study results. Despite this restriction, treatment rankings can still be produced as well as recommendations for construction and replication of treatment systems. The assumptions required for extrapolation of study data are as follows:

- A small test track in a single location will produce results representative of a larger road system,
- Confining materials will not influence the performance of different road treatments,
- Simulated parameters accurately represent natural events.

Agreement or disagreement with similar investigations will provide a metric for determining if these assumptions have been met, and if the data acquired can be applied to other spatial scenarios and temporal scales.

RESULTS

Hydrology

Turbidity

Turbidity sampled from all road sections ranged from 954 to 306,000 nephelometric turbidity units (NTU). The geotextile/geogrid treatment section with well-graded aggregate (WGG) produced the lowest maximum turbidity measured in each section, and the lowest minimum turbidity measured in each section. In contrast, the geotextile/geogrid treatment section with poorly-graded aggregate (PGG) produced the greatest maximum turbidity measured in each section, and the greatest minimum turbidity measured in each section (Table 4).

Treatment	WGC	WGB	WGG	PGG	PGB	PGC
Minimum	2,412	2,130	954	22,761	6,246	1,242
Maximum	295,974	239,598	156,735	306,180	234,009	222,102

Table 4: Minima and Maxima turbidity measurements (NTU) for each road section over the full duration of 600 truck passes.

The full time series of turbidity data is shown in Figure 5 and Figure 6 where turbidity is grouped by both treatment type and aggregate variety. The time series displays strong periodicity for every 100 truck passes, corresponding to the time when truck traffic was stopped for measurement of rutting. Within each period, turbidity typically increases with the number of truck passes.

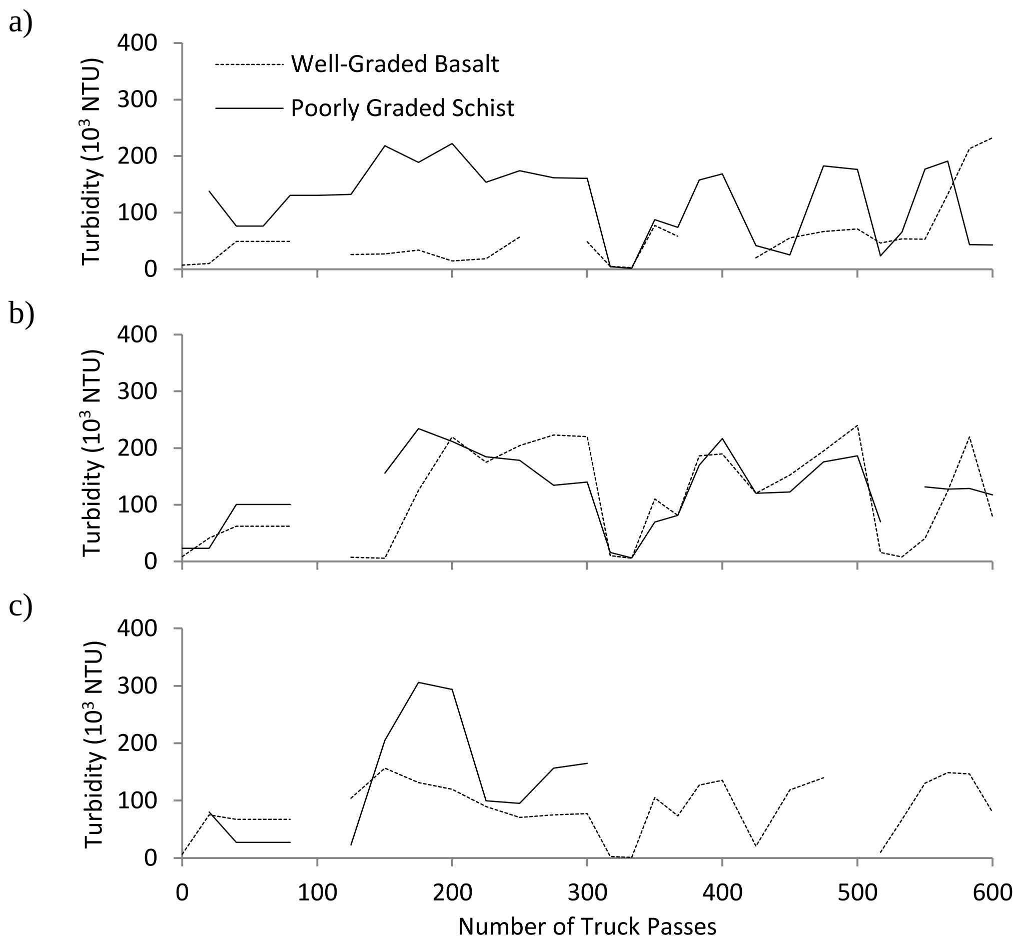

Figure 5: Measured turbidity in road runoff grouped by (a) control treatment sections, (b) biomass berm treatment sections, and (c) geotextile/geogrid treatment sections of well-graded and poorly-graded aggregate as a function of loading (truck passes).

Gaps in the time series data indicates a sample omission. Reasons for omitting a sample include not enough water in the ditch (no sample), not enough water in the sample bottle (sample size was insufficient for data analysis), or a sampling error (human error). During the last 300 truck passes, the PGG treatment section did not produce any measureable runoff. This indicates likely subsurface flume failure, although the failure mechanism was not physically apparent during field testing.

In the control treatment sections, the well-graded aggregate consistently produced less turbid effluent than the poorly-graded aggregate until the end of the test. This trend was not apparent or was inconsistent in the biomass and geotextile treatment sections.

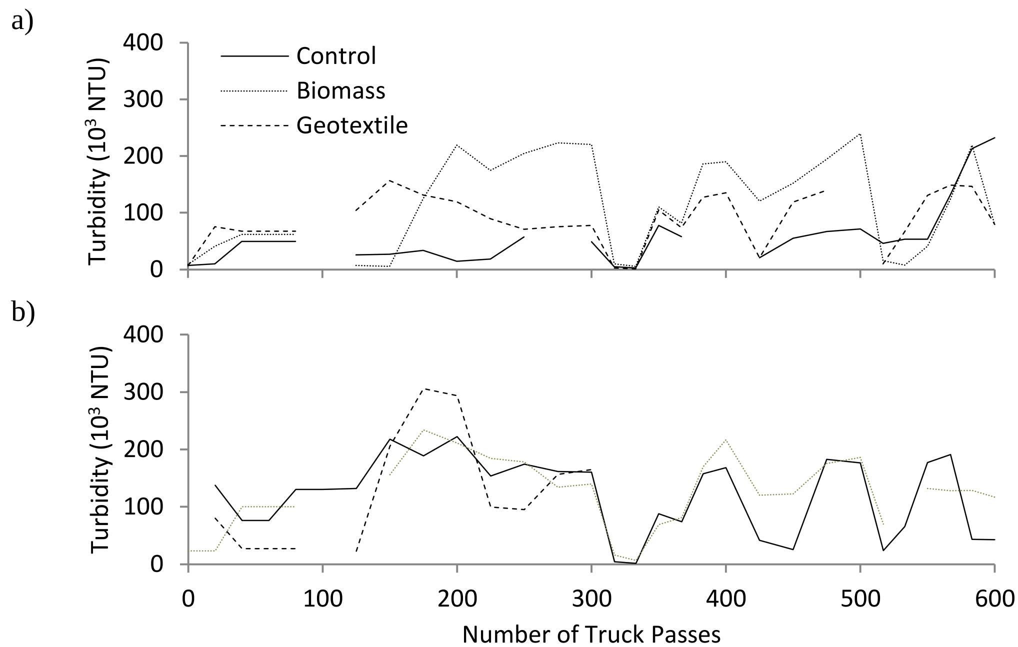

Figure 6: Measured turbidity in road runoff grouped by (a) well-graded aggregate and, (b) poorly-graded aggregate for all three road treatments as a function of loading (truck passes).

Field observations during testing noted lateral spreading of the aggregate layer, resulting in failure of the filter treatment systems by suspension of displacement. Specifically, aggregate spreading dislodged filter berms from their original position and road runoff was observed flowing under the filter treatment systems along the impermeable channel liner of the runoff collection flume. No mechanism was in place to quantify the amount of runoff bypassing the filtration systems, however this trend appeared to increase throughout testing in conjunction with the lateral spreading of the aggregate.

Suspended Solids

Suspended solids concentration (SSC) among all road section samples ranged from 439 to 297,000 g/L. The PGC treatment section had the lowest minimum SSC value. The PGB treatment section had the lowest maximum SSC value. The PGG treatment section had the highest minimum SSC value and the WGB treatment section had the highest maximum SSC value. By average values, the well-graded aggregate produced the highest and lowest sediment concentrations in the ditch runoff, while the poorly-graded aggregate had a lower range of sediment concentrations in the ditch runoff. These results can be found in Table 5.

Treatment	WGC	WGB	WGG	PGG	PGB	PGC
Minimum	2,070	900	448	8,460	3,760	439
Maximum	260,000	297,000	116,000	145,260	96,600	102,000

Table 5: Minima and Maxima SSC measurements (mg/L) for each road section over the full duration of 600 truck passes.

The full time series of SSC data is shown in Figure 7 and Figure 8 where SSC is grouped by both treatment type and aggregate variety. The time series displays periodicity for every 100 truck passes corresponding to the time when truck traffic stopped so road rutting measurements could take place. This trend is more apparent during the last 300 truck passes.

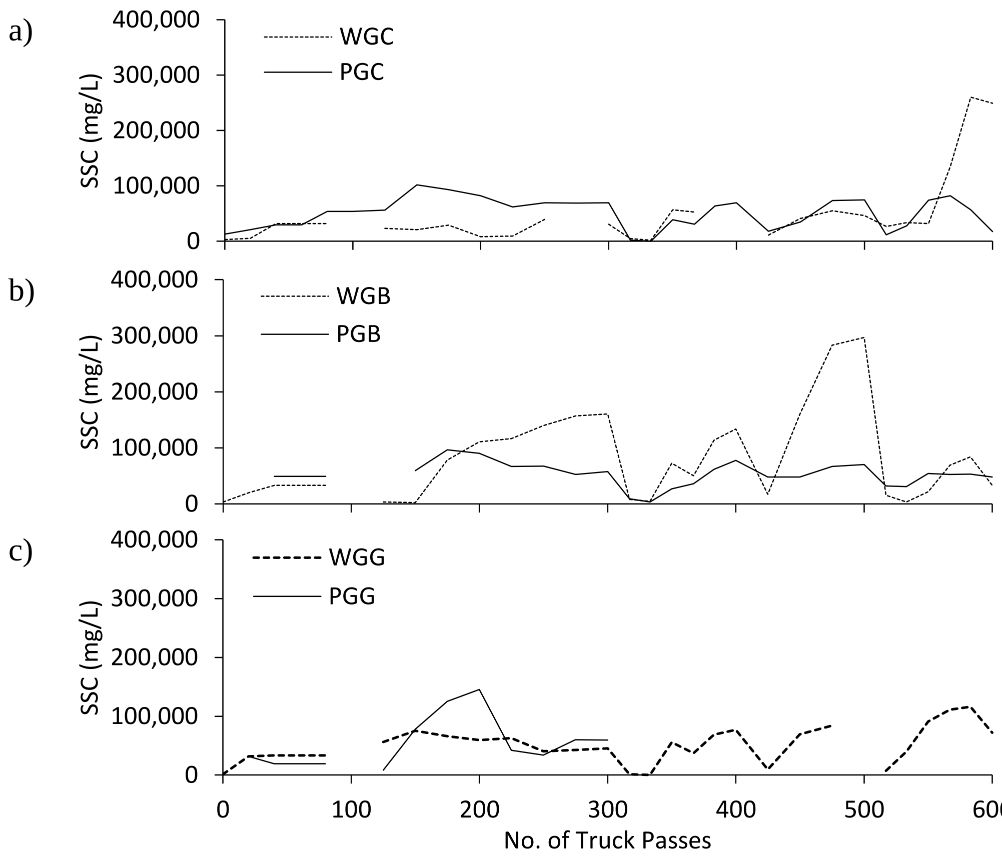

Figure 7: Measured SSC in road runoff grouped by (a) control treatment sections, (b) biomass berm treatment sections, and (c) geotextile/geogrid treatment sections of well-graded and poorly-graded aggregate as a function of loading (truck passes).

Similar to turbidity, there are also gaps in the time series data. These gaps are due to sample omission. As with turbidity data, reasons for omitting a sample include not enough water in the ditch (no sample), not enough water in the sample bottle (sample size was insufficient for data analysis), or a sampling error (human error).

With few exceptions, the same samples were used to test both turbidity and SSC; because of this, the PGG treatment section has neither turbidity nor SSC data during the last 300 truck passes when the section failed to produce road runoff.

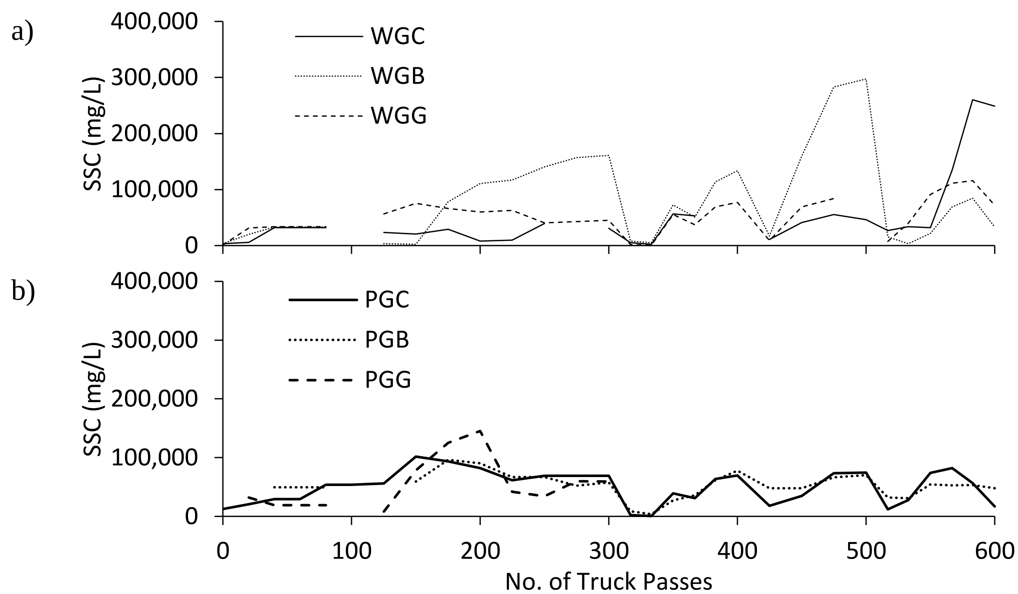

Figure 8: Measured SSC in road runoff grouped by (a) well-graded aggregate and, (b) poorly-graded aggregate for all three road treatments as a function of loading (truck passes).

For both well-graded and poorly-graded aggregate varieties, the control treatment sections (WGC and PGC) typically exhibited lower peak turbidity during each round of 100 truck passes.

Rainfall

During the first 300 truck passes, rain gauges were placed in the center of the road to measure the rate of simulated precipitation on the road. The gauges were read and rainfall depths recorded for every 48, 100, 200, and 300 passes, corresponding to the times when sprinklers were turned on and off. Table 6 shows the measured rainfall in each treatment section.

No. of truck passes	0 – 48	49 – 100	101 – 200	201 – 300
Rainfall duration (min)	55	20	35	30
	Rain gauge depths (mm)			
WGC	12	3	NA	NA
WGB	NA	6	NA	NA
WGG	21	4	NA	10
PGG	11	5	6	4
PGB	16	2*	7	9
PGC	16	5	4	10
Average depth (mm)	15	5	6	8
Average intensity (mm/hr)	17	14	10	17
Average rainfall intensity of all road sections = 15 mm/hr (0.6 in/hr)				

Table 6: Simulated rainfall intensity measurements during the first 300 truck passes. "NA" indicates rain gauge tipped over or was broken during testing. * indicates rain gauge was slanted therefore measurement was excluded from calculations.

Periodicity seen in the turbidity and SSC time series data shows a flushing effect from the simulated rainfall after traffic ceased. Runoff continued to transport sediment from the roadway after rainfall was discontinued. This flushing effect reduced the available solid material in the road prism; thus, when traffic re-started, initial turbidity and SSC readings start low, but increase rapidly after traffic passes.

After 600 truck passes, simulated rainfall ran for forty additional minutes and four additional runoff samples were taken to quantify the flushing effect seen in each treatment section. The WGG treatment section exhibited the lowest average turbidity during the flushing period. The WGB treatment section exhibited the lowest SSC value during the flushing period. The WGC treatment section exhibited the highest turbidity and SSC values during flushing. This is also the section that experienced the greatest level of road failure from rutting and lateral spread. All test sections show rapid reductions in turbidity and SSC during the flushing period (Figure 9).

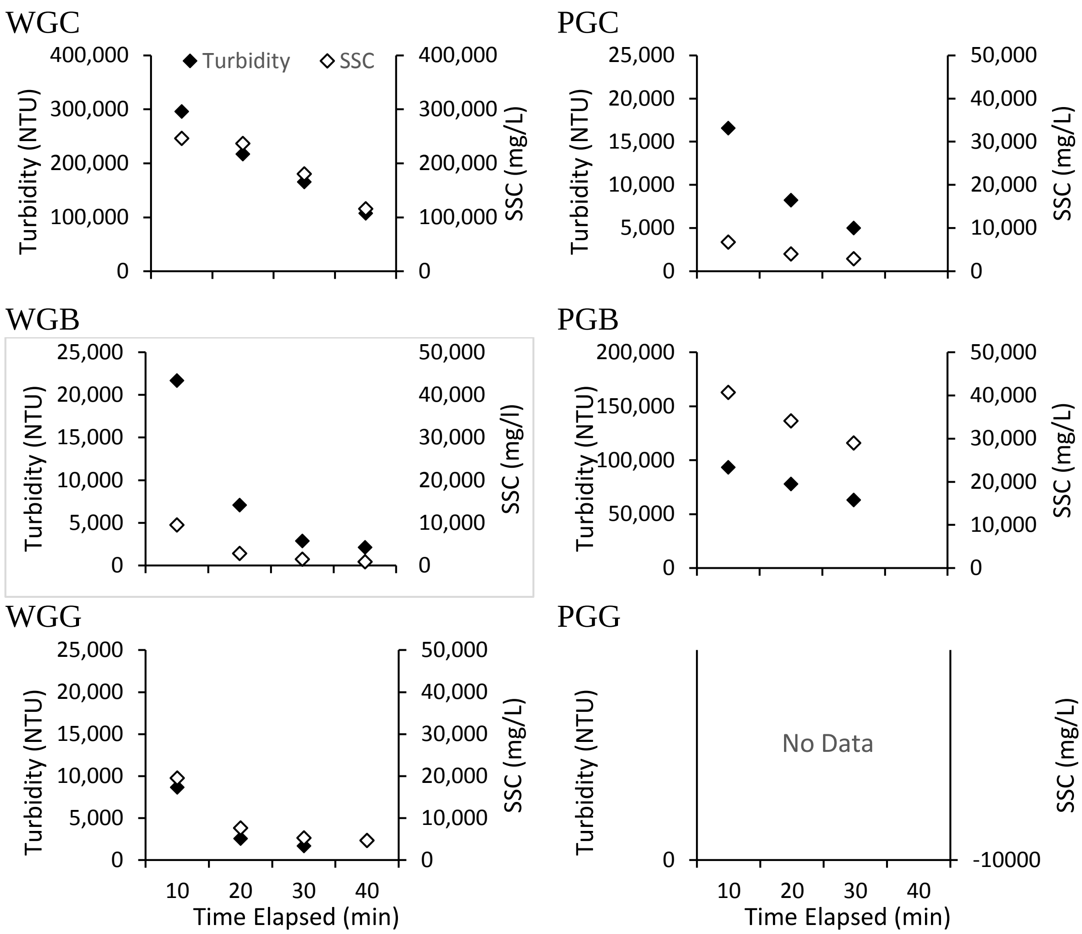

Figure 9: Turbidity and SSC sampled for 40 minutes after termination of truck traffic while simulated rainfall continued.

Permeability and Filtration

Laboratory tests were performed to determine the filtration benefits of the filter sand and geotextile wrap when loaded with turbid influent. The filter sand acting alone produced a minimum turbidity reduction of 67 %. When coupled with the geotextile used in the construction berm the minimum turbidity reduction increased to 74%. These data are derived from four different trials. Details provided in Table 7.

Filtration Treatment	Filter Sand Only		Filter Sand and Geotextile	
Influent Treatment	2 % SSC	1 % Fines	2 % SSC	1 % Fines
Influent Turbidity (NTU)	6,600	5,800	6,600	5,800
Maximum Turbidity (NTU)	2,200	1,500	1,200	1,500
Minimum Turbidity Reduction	67 %	75 %	82 %	74 %
Time to Peak Concentration (min)	8	5	5	10

Table 7: Summary of permeameter filtration tests.

Turbidity levels chosen for permeameter testing represent those found in road ditch runoff during sub-annual storms in the Oregon Coast Range (Miller 2014). The first two trials performed used an influent material of 2 % SSC by mass using solids recovered from the ditch samples (Figure 10). Although a grain size analysis was not performed on this material, the texture of the solids indicated particle sizes ranging from sand to fines. After 12 minutes, the 2 % SSC influent had clogged the permeameter hoses and prevented flow through the sand column. The third and fourth trials performed used an influent material of 1 % SSC by mass of only fine particles in the influent to avoid clogging of the device. The fine particles suspended well in the permeameter tubes allowing both a 20 minute sediment loading phase, and a 20 minute sediment flushing phase to take place (Figure 11).

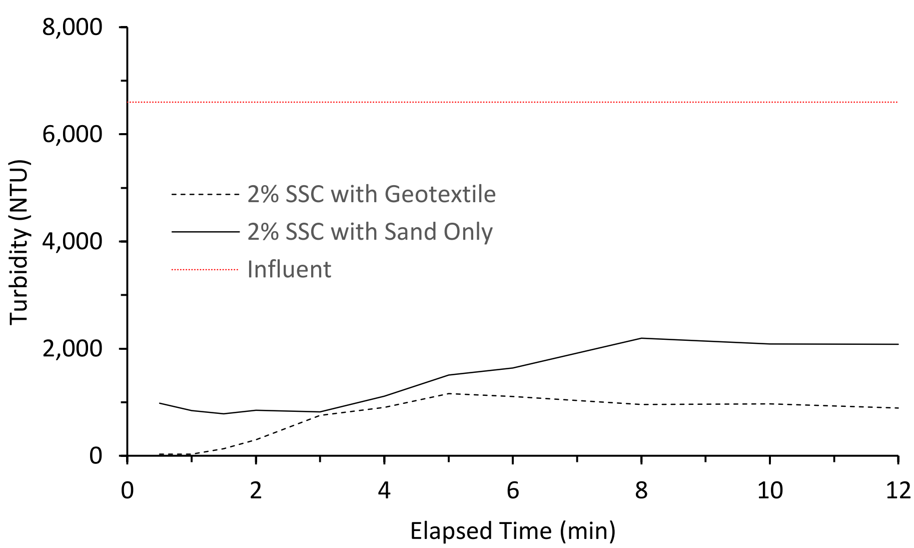

Figure 10: Permeameter trial time series using 2 % SSC by mass influent.

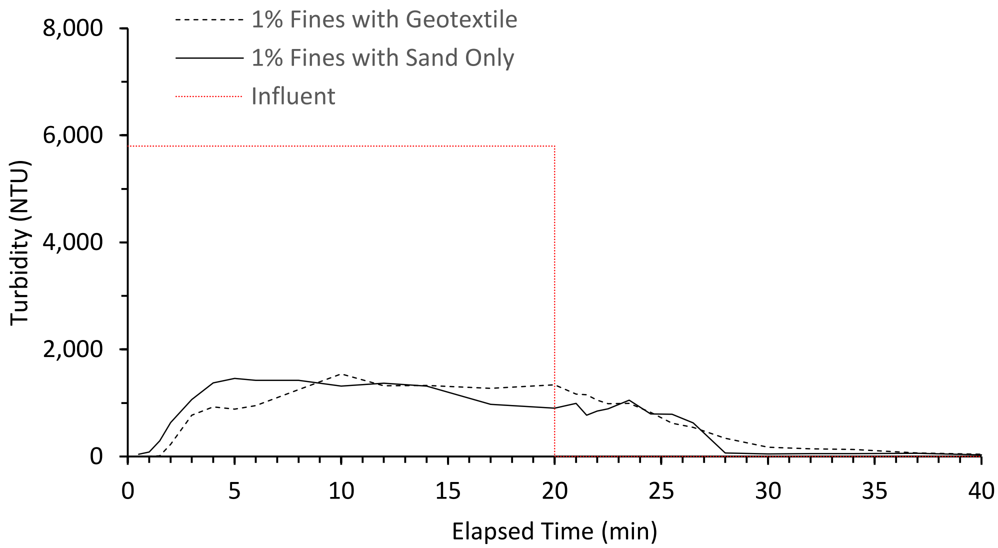

Figure 11: Permeameter trial time series using 1 % SSC fines by mass influent. The dotted vertical line separates the loading phase (turbid influent) vs. flushing phase (clean influent) effluent samples.

All permeameter tests revealed that peak concentration of effluent was achieved prior to any system flushing that occurred (only 1 % SSC Fines trials were flushed). This is a possible indicator that the volume of voids in the filter sand needed to be reduced to achieve maximum filtration benefit. For all trials, this took no more than 10 minutes to achieve. During the 2% SSC trial using the geotextile, the time to peak concentration occurred soon before that of the 2 % SSC trial using filter sand only, however the peak concentration of the geotextile-treated effluent was nearly half that of the filter sand only effluent (Figure 10). The 1 % SSC Fines trials shows a reduction in time to peak concentration with use of the geotextile filter but no significant difference in maximum turbidity. In the flushing stage of the 1 % SSC Fines trials, both treatments returned to near-initial turbidity values after 20 minutes (Figure 11).

Aggregate Performance

Changes in Gradation

Both the well-graded and poorly-graded aggregate varieties displayed quantifiable signs of degradation under traffic loading, producing fine materials from the breakdown of larger grain sizes (See Appendices D and E for particle size distribution tables). Figure

12 shows an increase in fine materials produced as a function of truck traffic. For the average gradation of the poorly-graded aggregate, the rate of change in fine particles appears to increase as a function of truck traffic. It should be noted, however, that the grain size distributions shown in Figure 12 are the results of averages from the aggregate samples tested after 100 (batch 1), 300 (batch 2), and 600 (batch 3) truck passes. Variability among aggregate samples may influence this relationship.

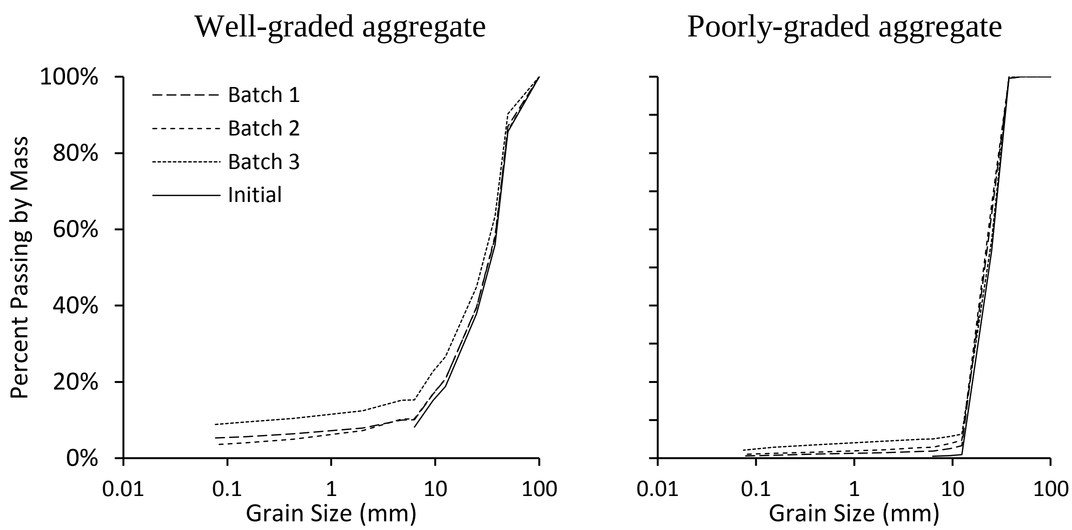

Figure 12: Changes in gradation from initial aggregate sample. Batch 1 includes averages of aggregate samples after 100 truck passes, Batch 2 includes averages of aggregate samples after 300 truck passes, and Batch 3 includes averages of aggregate samples after 600 truck passes.

Measurement of particle breakage using techniques from Hardin (1985) provides a means of comparing the quantity of degradation both between aggregate varieties and among sample batches (number of truck passes). The results from Table 8 show that the well-graded aggregate exhibited greater relative breakage throughout testing than the poorly-graded aggregate. The well-graded aggregate also experienced a wider range of relative breakage throughout testing.

Treatment	Batch 1	Batch 2	Batch 3
WGC	0.041	0.028	0.103
WGB	0.017	0.032	0.039
WGG	0.038	0.031	0.083
Averages	0.032	0.030	0.075
PGC	0.020	0.037	0.075
PGB	0.027	0.038	0.054
PGG	0.017	0.029	0.035
Averages	0.021	0.035	0.055

Table 8: Hardin relative breakage values for each aggregate separation bag.

The poorly-graded aggregate shows breakage trends with truck traffic and with road treatment. All poorly-graded test sections experienced increased relative breakage as a result of increased truck traffic. Among batches of poorly-graded aggregate, the geotextile/geogrid treatment section had the lowest relative breakage. These trends were not apparent in the well-graded aggregate sections, although the well-graded aggregate did experience the greatest relative breakage after 600 truck passes.

Relative breakage trends reflect the breakage among particle sizes analysis. In this case, only particle sizes down to ¼" were analyzed using Hardin's procedure. Therefore it is important to note that trends in relative breakage do not necessarily represent particle sizes smaller than ¼"—those particle sizes which may be suspended in runoff and transported from the road surface.

Subgrade Stress

Subgrade stress increased in each test section throughout testing. The WGC treatment section exhibited the highest level of subgrade stress and the PGB treatment section exhibited the lowest level of subgrade stress. During field testing, the WGC section experienced the greatest lateral spreading as noted in Table 9, indicative of higher stress concentrations encountered at the subgrade. The reduced aggregate thickness is attributed to the large subgrade stresses recorded. In contrast, the pressure cell in the PGB section was buried outside the center of the wheel track of the road, the result of minor road realignment during construction. Due to the anomalies in these two sections, analysis of subgrade stress and pressure cell data excludes these sections. Figure 13 shows all six test sections and clearly illustrates the extreme subgrade stress seen in the WGC section and the consistently low subgrade stress of the PGB section. Although all road sections did experience some form of lateral spreading, sections WGB, WGG, PGG, and PGC experienced similar lateral spreading and contained pressure cells all located directly under the wheel tracks of the road.

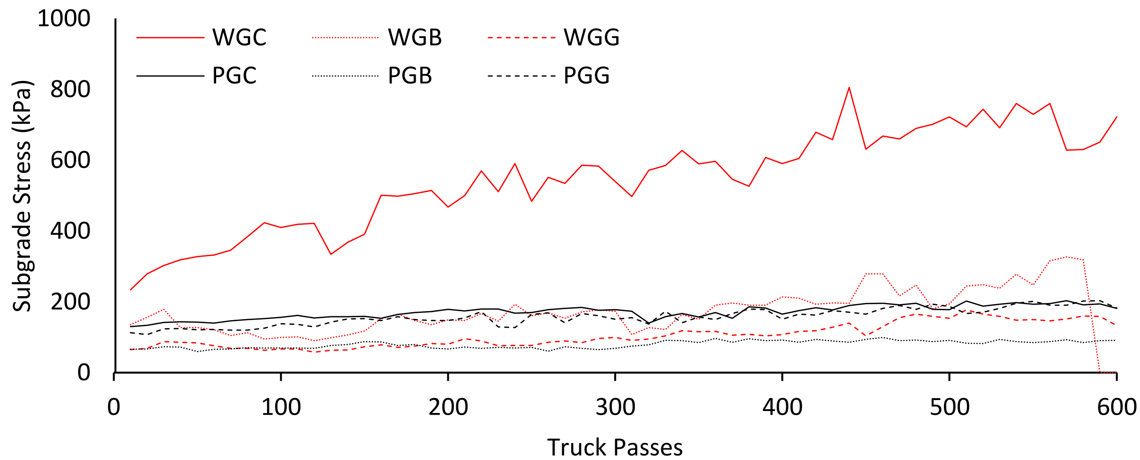

Figure 13: Maximum subgrade pressure per truck pass (0 to 600 truck passes) for all test sections.

Trends in Figure 13 are difficult to discern however both geogrid reinforcement sections provided a reduction in subgrade stress for either aggregate variety. Another trend seen from the pressure data reveals that the well-graded aggregate was more effective at distributing loads than the poorly-graded aggregate, even with geogrid reinforcement, during the first 300 truck passes. Figure 14 shows both these trends more clearly by eliminating the WGC and PGB section from the graph. It should be noted that both Figure 13 and Figure 14 show only the maximum stress produced every 10 truck cycles. The reason for this is to capture a) truck passes moving directly over pressure cells, and b) a coarser temporal resolution which more clearly shows trends in the data. For a full plot of all 600 readings for all 6 test sections, see Appendix H.

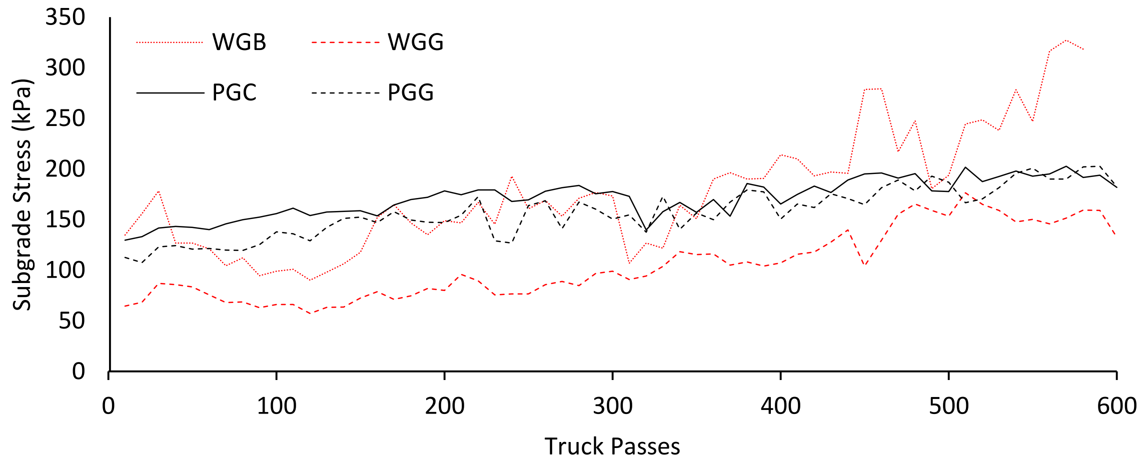

Figure 14: 10-cycle max subgrade pressure for non-anomalous treatment sections.

Truck traffic produced a moderate increase on subgrade stress in all test sections except the WGC treatment section which experienced a rapid increase in subgrade stress. Not only did the WGC section experience the largest subgrade stresses but the subgrade stresses increased at a greater rate than other test sections throughout testing (Figure 13).

Rutting

Each test section presented wheel rutting and subsequent lateral spreading. Ponding of water was present in deep ruts but no overland flow was observed. Rutting was measured after the first 50 truck passes and after each 100 truck passes (cumulative) thereafter. Upon completion of the first day of testing (300 truck passes) lateral spreading on the inboard side of the road, particularly in the WGC treatment section, prevented further rutting measurements to be taken from the inboard wheel well. During the second day of testing (final 300 truck passes), rutting was measured from the outer wheel wells of the road which experienced less lateral spread due to increased resistance stemming from the insloped road prism. Rutting measurements are listed in Table 9 and Table 10 and rutting geometry is shown in Figure 15 and Figure 16 where the rutting depths for the control and biomass berm treatment sections are averaged in order to compare rutting with and without the geogrid reinforcement.

Rutting - Inside Wheel Track (mm)													
48 Passes		WGC		WGB		WGG		PGG		PGB		PGC	
	Section	1A	1B	2A	2B	3A	3B	4A	4B	5A	5B	6A	6B
Distance from CL (mm)	0	0	0	0	0	0	0	0	0	0	0	0	0
	300	15	7	17	20	10	13	15	29	22	21	21	22
	600	20	20	37	37	10	17	17	30	26	31	22	31
	900	26	21	40	45	13	21	36	40	30	37	15	0
	1200	0	0	0	0	0	0	0	0	0	0	0	0
100 Passes		WGC		WGB		WGG		PGG		PGB		PGC	
	Section	1A	1B	2A	2B	3A	3B	4A	4B	5A	5B	6A	6B
Distance from CL (mm)	0	0	0	0	0	0	0	0	0	0	0	0	0
	300	18	12	34	11	21	14	22		25	27	22	20
	600	24	37	70	31	36	35	49		33	37	26	38
	900	46	45	77	48	45	48	80		44	51	28	40
	1200	0	0	0	0	0	0	0	0	0	0	0	0
200 Passes		WGC		WGB		WGG		PGG		PGB		PGC	
	Section	1A	1B	2A	2B	3A	3B	4A	4B	5A	5B	6A	6B
Distance from CL (mm)	0	0	0	0	0	0	0	0	0	0	0	0	0
	300	18	38	70	65	20	50	50	57	39	40	26	17
	600	55	57	110	100	41	70	60	85	44	41	37	30
	900	65	80	112	118	70	58	71	91	52	35	57	32
	1200	0	0	0	0	0	0	0	0	0	0	60	0
300 Passes		WGC		WGB		WGG		PGG		PGB		PGC	
	Section	1A	1B	2A	2B	3A	3B	4A	4B	5A	5B	6A	6B
Distance from CL (mm)	0	0	0	0	0	0	0	0	0	0	0	0	0
	300	31	45	82	67	45	50	77	68	38	47	28	41
	600	70	74	143	157	75	75	97	108	58	51	58	54
	900	75	97	183	180	84	88	102	108	62	48	62	60
	1200	0	0	0	0	0	0	0	0	0	0	69	32

Table 9: Rutting measurements for the inboard wheel track measured at 48, 100, 200, and 300 truck passes.

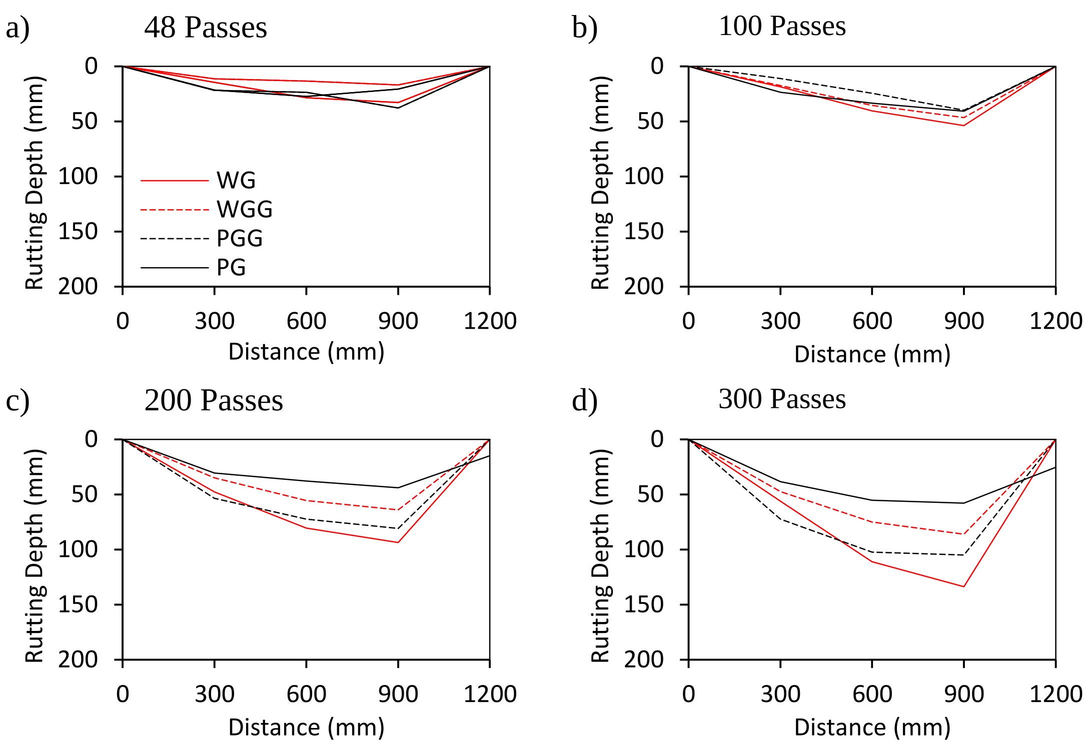

Figure 15: Inboard wheel track rutting from 48 to 300 truck passes for well graded aggregate without reinforcement (WG, averaged), well-graded aggregate with geogrid reinforcement (WGG), poorly-graded aggregate without reinforcement (PG, averaged), and poorly-graded aggregate with geogrid reinforcement (PGG).

During the first 300 truck passes, the inboard wheel tracks exhibited rutting that increased with the number of truck passes. The well-graded aggregate with no geogrid reinforcement experienced the greatest rutting at 183 mm (7.2 inches) of depth and the poorly-graded aggregate with no geogrid reinforcement experiences the least amount of rutting at 51 mm (2.0 inches) after 300 total truck passes (Table 9).

During the last 300 truck passes, all wheel tracks exhibited substantial lateral spreading. The uppermost inboard wheel tracks (sections 1 and 2) spread laterally into the inboard ditch. This prevented consistent measurement of inboard wheel track rutting and therefore only the outer wheel tracks were measured for rutting for 300 to 600 truck passes. The lateral spreading present increased the rut measurement transect width to 1800 mm (72 inches). Only one rutting measurement was taken per section during the last 300 truck passes (Figure 16).

Rutting - Outside Wheel Track (mm)							
300 Passes		WGC	WGB	WGG	PGG	PGB	PGC
	Section	1A	2A	3A	4A	5A	6A
Distance from CL (mm)	0	0	0	0	0	0	0
	300	5	16	7	20	0	0
	600	24	36	37	21	16	21
	900	30	36	41	22	47	21
	1200	42	16	46	34	61	26
	1500	25	3	17	11	77	34
	1800	0	0	0	0	0	0
400 Passes		WGC	WGB	WGG	PGG	PGB	PGC
	Section	1A	2A	3A	4A	5A	6A
Distance from CL (mm)	0	0	0	0	0	0	0
	300	10	0	19	50	25	22
	600	20	21	29	57	43	36
	900	26	51	35	64	49	56
	1200	29	80	45	23	23	58
	1500	0	88	5	25	0	0
	1800	0	0	0	0	0	0
500 Passes		WGC	WGB	WGG	PGG	PGB	PGC
	Section	1A	2A	3A	4A	5A	6A
Distance from CL (mm)	0	0	0	0	0	0	0
	300	15	5	19	18	20	20
	600	26	28	28	47	41	38
	900	48	62	36	64	41	55
	1200	30	81	45	68	32	58
	1500	7	102	18	6	0	0
	1800	0	0	0	0	0	0
600 Passes		WGC	WGB	WGG	PGG	PGB	PGC
	Section	1A	2A	3A	4A	5A	6A
Distance from CL (mm)	0	0	0	0	0	0	0
	300	7	29	17	19	20	8
	600	18	60	27	50	43	21
	900	29	86	35	67	55	38
	1200	35	111	44	87	26	61
	1500	26	0	22	7	9	59
	1800	4	0	0	0	11	0

Table 10: Rutting measurements for the outer wheel track measured at 300, 400, 500, and 600 truck passes.

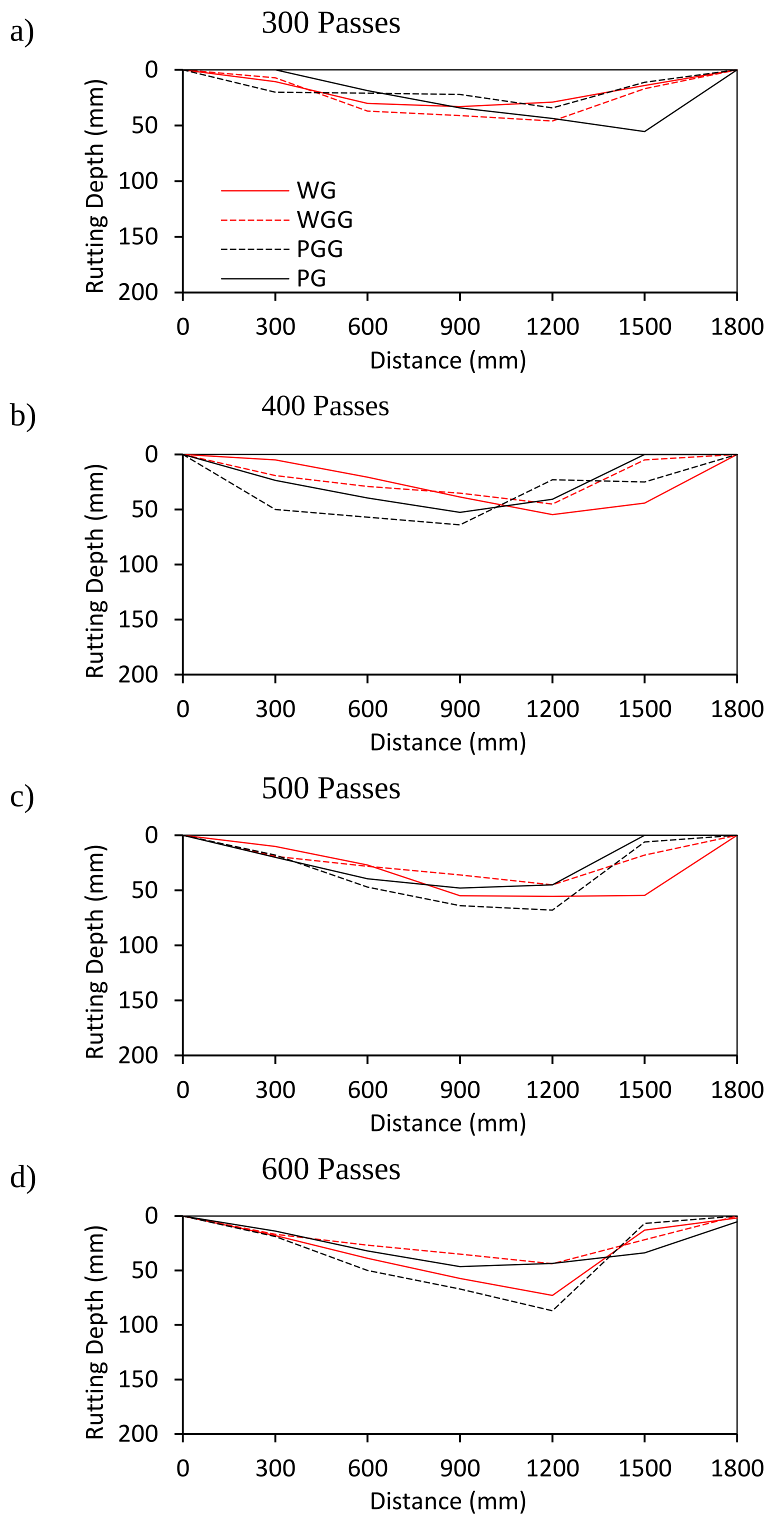

Figure 16: Outer wheel track rutting from 300 to 600 truck passes for well graded aggregate without reinforcement (WG, averaged), well-graded aggregate with geogrid reinforcement (WGG), poorly-graded aggregate without reinforcement (PG, averaged), and poorly-graded aggregate with geogrid reinforcement (PGG).

The outer wheel track rutting exhibited different trends and geometry from the inboard wheel track. After 300 truck passes, both wheel tracks experienced substantial lateral spreading but the outer wheel track maintained a consistent level of integrity to allow measurement during the final 300 truck passes. The outer wheel rut with the greatest depth after 600 passes was the well-graded aggregate (biomass section) at 111 mm (4.4 inches) and the outer wheel rut with the lowest depth after 600 passes was also the well-graded aggregate (control section) at 35 mm (1.4 inches) both shown in Table 10. Despite high variability in rutting depths among similar test sections, all rutting increases with the number of truck passes (Figure 17 and Figure 18).

Figure 17 and Figure 18 show the rutting variation with traffic loading. The geogrid treatment sections for both well-graded and poorly-graded aggregates rutted less than their non-reinforced counterparts during the first 300 truck passes shown in Figure 17. This relationship is not apparent during the last 300 truck passes shown in Figure 18.

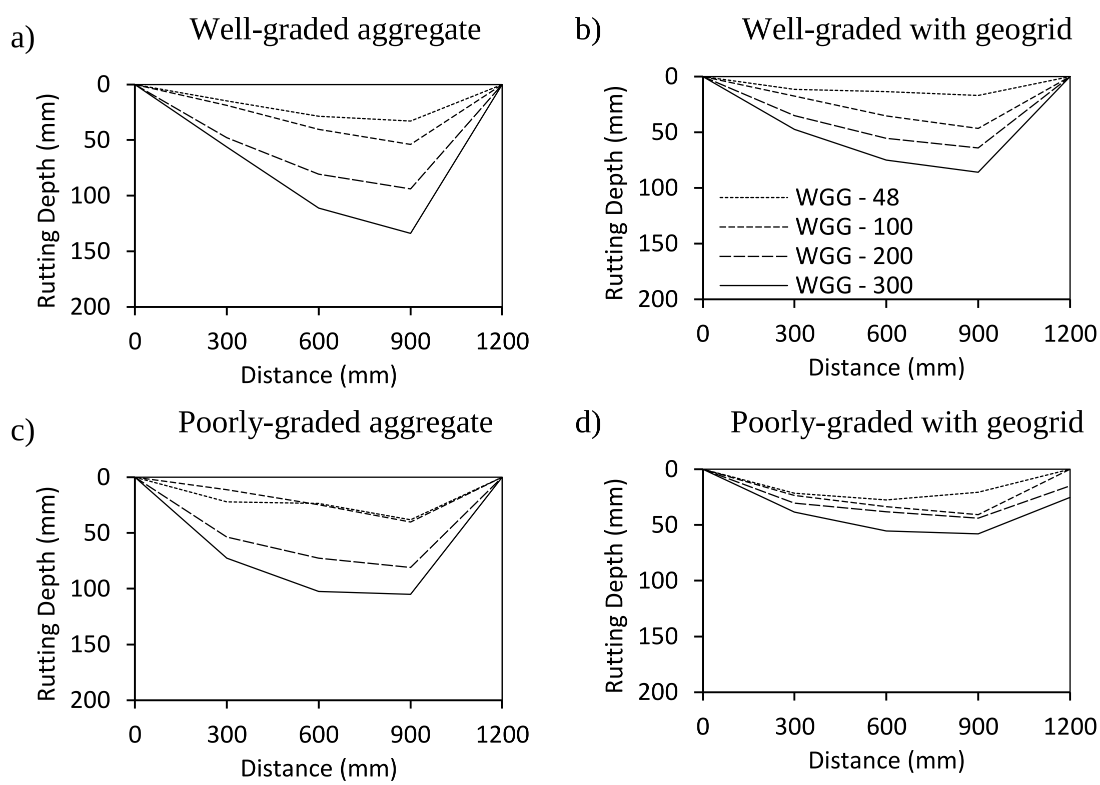

Figure 17: Inboard wheel track rutting depths at 48, 100, 200, and 300 truck passes segregated by treatment type.

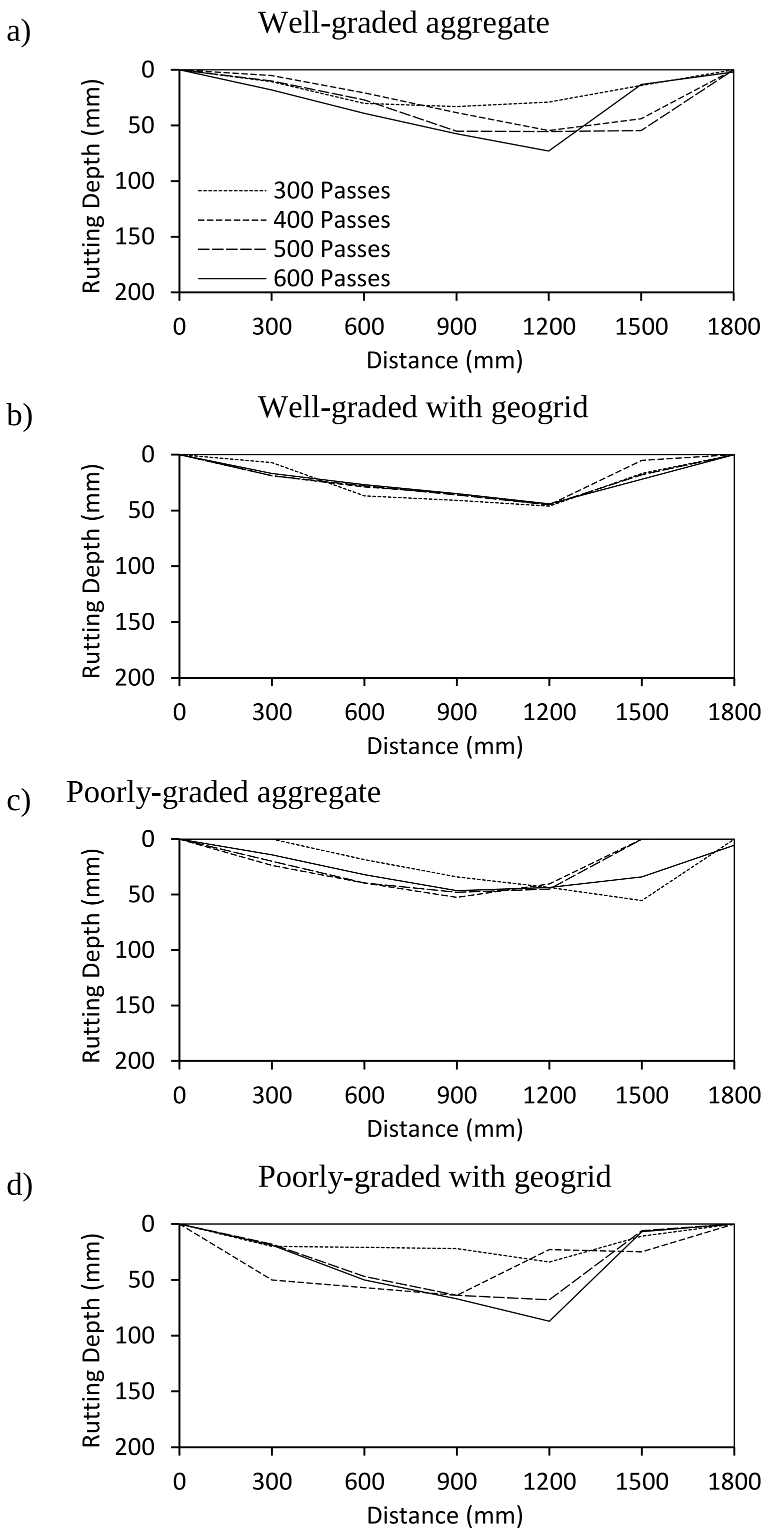

Figure 18: Outside wheel track rutting depths at 300, 400, 500, and 600 truck passes segregated by treatment type.

During the last 300 truck passes, lateral spreading was measured on the inside wheel track of the road. The spread of each rut was measured from a fixed wheel track centerline. It should be noted that the data in Table 11 are a reflection of lateral spread relative to the fixed wheel track and not necessarily at the center of each truck pass. Although the greatest measurement of lateral spreading occurred at 600 truck passes, Table 11 shows the rut and spread location changing over time with repeated loading.

	Road Section Treatment					
Truck Passes	WGC	WGB	WGG	PGG	PGB	PGC
300	280	270	190	190	170	150
400	270	470	240	320	200	200
500	140	500	270	390	220	180
600	330	560	320	470	270	230

Table 11: Average lateral spreading per section as measured from the centerline of the inner wheel track towards the ditch. All measurements are in mm.

DISCUSSION

Evaluation of Treatment Methods

Findings from this investigation are consistent with pre-established relationships from other studies. Agreement with similar studies validates the construction techniques and parameter constraint employed in this study and is one way of showing the representative functionality of the system was not compromised by construction or confinement techniques. Although there is evidence that the channel liner material prevented proper interlock between the aggregate and the filter berms, the mechanics of the road and runoff systems have not been impaired. Expected relationships such as the linear correlation between turbidity and SSC provide evidence that the techniques used to analyze the data were appropriate and did not violate known relationships.

Sediment Generation

Changes in particle size distribution from exhumation bags revealed the amount of sediment produced in each section of the road prism. Due to the experimental set up this study, fine material (particles passing ASTM No. 200 sieve) generation was not explicitly measured due to the destructive nature of the wet sieving procedure. Fine material was, however, measured in each aggregate separation bag once removed from the roadway, and the change in particles smaller than 6.3 mm (0.25 inches) was quantified for each aggregate separation bag (See Appendices D and E for aggregate bag gradation before and after testing).

Fine sediment material was produced as a function of truck traffic. Vehicular loading caused aggregate particles in both the well-graded and poorly-graded aggregates to break down into smaller particle sizes. Figure 12 shows an increase in fine materials present in both aggregate varieties. Also apparent is the increased rate of change of particle sizes smaller than 10 mm (0.39 inches) in the poorly-graded aggregate samples.

An interesting trend in the breakage of each aggregate variety was the higher relative breakage of the well-graded aggregate (Table 8). The poorly-graded aggregate contained more void spaces and had less surface area contact between particles to distribute loading however it experienced less relative breakage and a lower range of relative breakage throughout time then the well-graded aggregate.

When comparing relative breakage within batches and among aggregate varieties, the poorly-graded geogrid treatment section consistently had lower relative breakage than its poorly-graded counterparts throughout the duration of testing. This trend was not apparent for well-graded aggregate, however increased truck traffic (600 passes) produced the highest relative breakage all treatment sections.

The geogrid reinforcement improved the load distribution over the native subgrade material. Subgrade pressure data indicates the geogrid reinforcement provided a benefit in load distribution, however rutting measurements show increased rutting in the PGG treatment section. (Figure 18). The geogrid reinforcement benefited the well-graded aggregate, while it produced greater rutting depths in the poorly-graded aggregate. This is noticeably linked to the lateral spreading (Table 11). The greatest lateral spreading in the poorly-graded aggregate material occurred in the geogrid treatment section which reduced the aggregate layer thickness, thus inhibiting its ability to distribute traffic loading. It is difficult to determine whether or not the geogrid played a role in the increased lateral spreading of the PGG treatment section.

Sediment Delivery

Total sediment load was not quantified in this study, therefore sediment yield is quantified by peak sediment loads through time. Due to the periodicity in the data caused by the truck traffic, the maximum turbidity during each 100 truck passes was plotted in Figure 19 and Figure 20. Maximum turbidity produced in each section during each round of truck passes is an indicator of total sediment yield (Lewis 1996) and can be used to compare road segments. Treatment sections are grouped by both treatment type (Figure 19) and aggregate variety (Figure 20) for comparison.

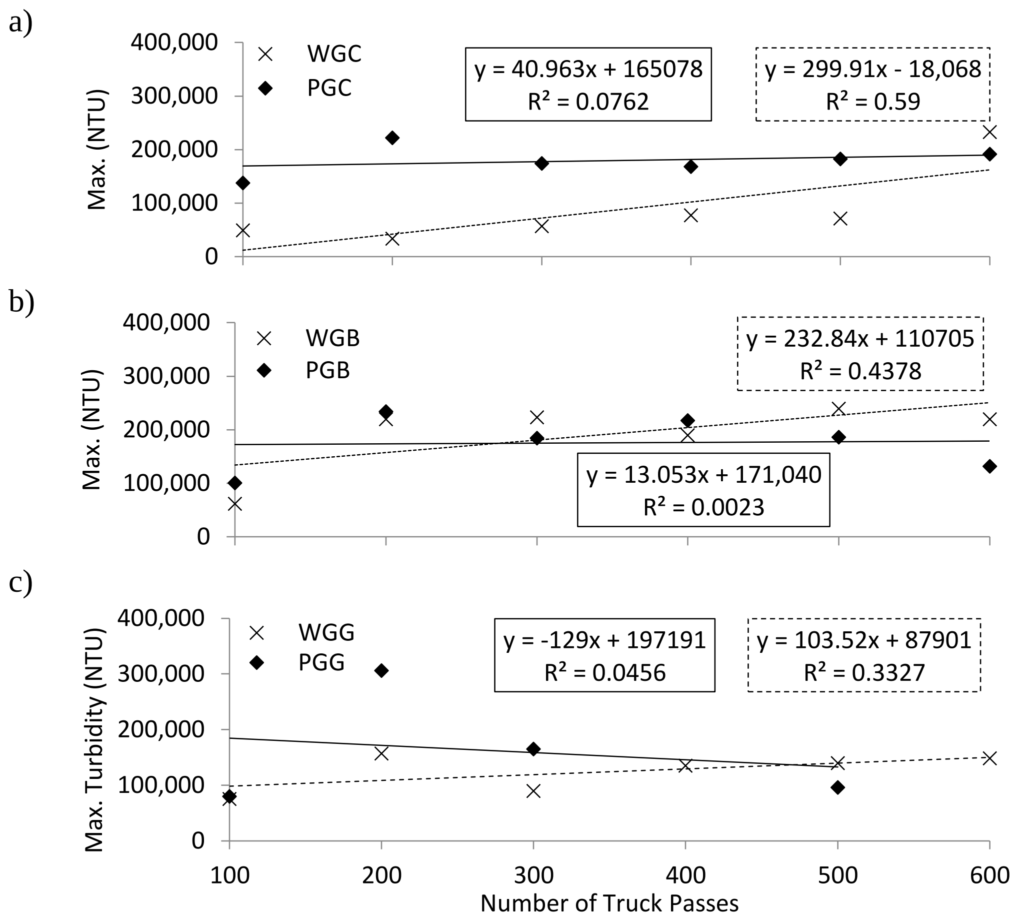

Figure 19: Maximum 100-cycle turbidity in road runoff grouped by (a) control treatment sections, (b) biomass berm treatment sections, and (c) geotextile/geogrid treatment sections of well-graded and poorly-graded aggregate as a function of loading (truck passes).

The data in Figure 19 indicate that the poorly-graded aggregate produced more turbid runoff than the well-graded aggregate in the control sections while both aggregate varieties produced similar amounts of turbidity in runoff in the biomass treatment section. A linear regression analysis of these relationships, however, reveals poor correlation coefficients for the well-graded aggregate and no discernable correlation for the poorly-graded aggregate. The limiting sample size and lack of replication also prevents statistically significant assertion of these relationships.

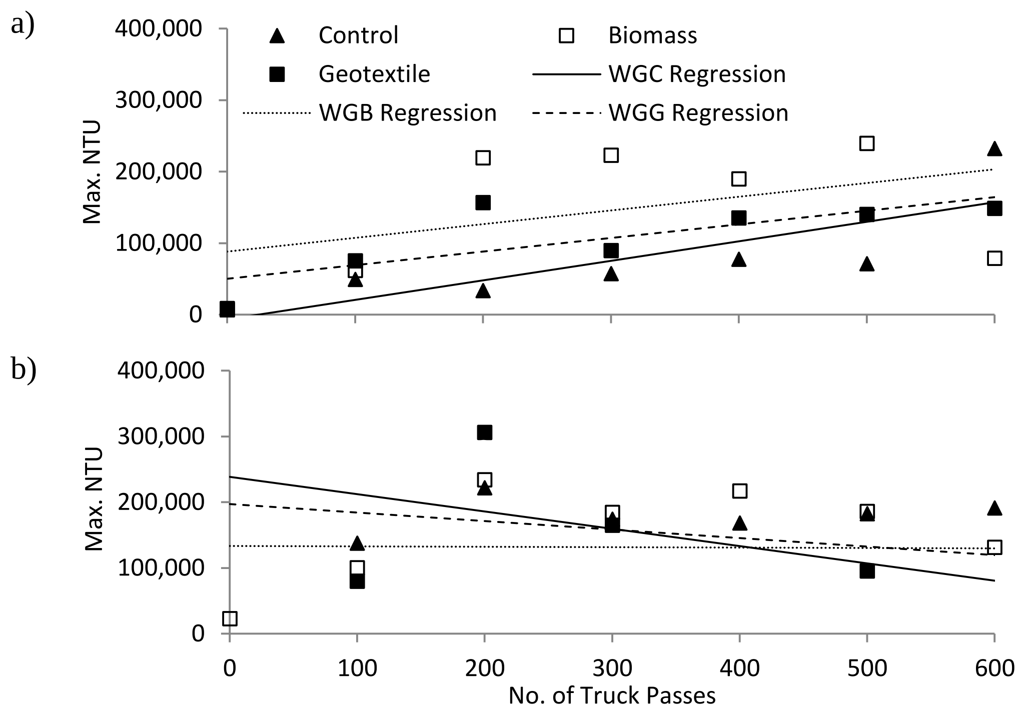

Figure 20: Maximum 100-cycle turbidity in road runoff grouped by (a) well-graded aggregate and, (b) poorly-graded aggregate for all three road treatments as a function of loading (truck passes).

Figure 20 shows a trend of increasing turbidity for the well-graded aggregate as the number of truck passes increases (R^2 values between 0.33 and 0.59). In contrast, the poorly-graded aggregate shows a trend of decreasing turbidity as the number of truck passes increases after the first 200 passes (R^2 values between 0.002 and 0.08). A possible explanation of these trends lies within the optimum fines content of the aggregate and the ability of fine material to fill voids, and dissipate the energy of the runoff. As the poorly-graded aggregate breaks apart and produces fine materials, the voids are filled in, lengthening the path water must flow to escape the road by routing the water around a greater and greater number of particles. This slows the velocity of water leaving the road and reduces the carrying capacity of the runoff. This trend is expected to continue until optimal fines content is achieved (Foltz and Truebe 2003). By the same logic, the increasing turbidity of the well-graded aggregate may be due to a higher-than-optimal fines content causing the road to flush excess fines in runoff until reaching an ideal fines content. In either case, the fit of the regression lines for these trends are poor, especially for the poorly-graded aggregate.

Sequestration Benefit

The geotextile filtration treatment was expected to produce effluent with the lowest turbidity. This expectation was only realized in the WGG section where the treatment was applied to well-graded aggregate (Table 4). It should be noted, however, that the PGG treatment section experienced some form of road failure such that road runoff during the last 300 truck passes was reduced to one measurable sample. This reduced the turbidity and SSC test sample size for this section by more than 50%. This makes analysis of the efficacy of the geotextile and filter sand berm treatment difficult to validate with only one data set. This prompted further testing of the geotextile and sand filter system in a lab.

Preliminary lab test results of the geotextile fabric and filter sand reveal that both the use of filter sand alone, and the use of filter sand with the geotextile wrap provide a substantial reduction in the turbidity of the effluent (Figure 10 and Figure 11). The first effluent sample in each test records the base level turbidity of water leaving the sand column. Although there is a large variability in the base level turbidity of each test, when allowed 20 minutes to flush the system, turbidity levels returned to near or below their base levels. When compared to the Oregon Department of Environmental Quality (DEQ) standards for turbidity in streams, the brief flushing period holds up well.

The current rule for total maximum daily load (TMDL) of turbidity in streams caps the increase at 10% of the naturally occurring (base level) turbidity (OAR 340-041-0036). Some disturbance activities, either for emergencies or other permitted operations, are allowed to discharge higher level turbidities into streams provided it is a short-duration event. The laboratory filtration tests were designed to simulate the immediate spike in turbidity caused by truck hauling on a wet aggregate surface. The 20-minute recovery time recorded in Trials 3 and 4 show how the filter sand not only reduces the turbidity of the effluent, but also returns the system to base-levels quickly.

Evaluation of the commercial viability of a treatment depends on the cost, ease of construction, and sediment sequestration benefit. Due to the labor required to construct a filter sand berm, this treatment is not feasible for long segments of forest roads. However, road segments that have been identified as major sediment sources or road-stream crossings would benefit from the sediment sequestration benefits of the sand berm. The reduction in peak turbidity and extended time to concentration of the geotextile and filter-sand combination make this prototype particularly viable for near-stream applications. Targeted application of this construction technique could provide a much needed reduction in effluent turbidity of forest roads, especially in light of trends towards stricter water quality standards for discharge into natural water bodies.

Unlike the geotextile wrap-faced sand berm, the biomass berm filtration systems did not provide a discernable treatment benefit over the course of 600 truck passes. Applied to the well-graded aggregate, the biomass berm produced the largest measurements of turbidity and SSC. Applied to the poorly-graded aggregate, the biomass berm produced turbidity and SSC values similar to those of the control segment. During field testing, road runoff in the biomass berm treatment sections was observed traveling under the berm and along the channel liner into the ditch sample bucket. Without having to flow through the berm or around interlocking aggregate, the biomass berm treatment created a preferential flow path for the road runoff exiting the road prism. While the omission of a channel liner in a commercial application of the biomass berm may eliminate the preferential flow path, the berms themselves did not appear to interlock well with the surrounding aggregate. This shortcoming and the addition to the labor intensive construction of the berm make this treatment option not viable for widespread use. Improved berm construction techniques may make the Douglas fir byproduct more feasible, but investigation of the effects of multiple construction techniques is outside the scope of this study.

Comparison to Contemporary investigations.

The turbidity and SSC data collected from ditch runoff is linearly correlated using simple linear regression similar to Lane and Sheridan (2002). Figure 21 shows the relationship between these two parameters from both control section data sets (only the control segments were used in the regression to avoid any influence by the filtration systems on this relationship).

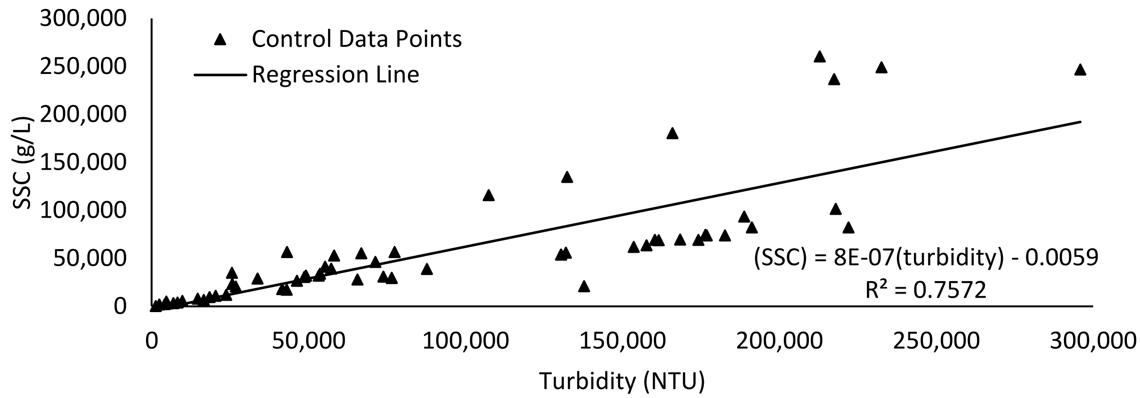

Figure 21: Linear regression relationship between SSC and turbidity from all 'control' treatment data.

Another familiar relationship portrayed in this study was the periodicity seen in turbidity and SSC as a result of intermittent simulated rainfall. As shown by Bilby, Sullivan, and Duncan (1989), truck traffic is the predominant driver of sediment generation in an unpaved road while rainfall is the predominant driver of sediment transport. Sediment levels in ditch runoff at the initiation of truck traffic were substantially less than the sediment that exited the road during repeated truck passes. When truck traffic ceased, the flushing effect of the rainfall on the road lowered turbidity and sediment levels to near-initial conditions as shown in Figure 9. This flushing pattern produced the periodicity seen in Figure 5 through Figure 8 when truck traffic paused every 100 cycles.

Lessons Learned

Data Variability

In search of relationships between sediment generation, sediment delivery, and aggregate performance, variability in the data prevented causal relationships from being established. One example of this is the rutting data, where the well-graded aggregate (WG) experienced the deepest rutting on the inboard wheel track while the poorly-graded aggregate with geogrid reinforcement (WGG) produced the deepest rutting on the outer wheel track of the road. To complicate matters, the unexpected level of lateral spreading in the road prevented the same wheel tracks from being measured throughout the full 600 truck passes. It is thus unclear whether or not the trends seen in the rutting of the road are due to the number of truck passes, or the location of the wheel track on the insloped road. To avoid ambiguity in interpretation of rutting results, future analyses should be performed on road that are either flat or crown-shaped.

Evaluation of Experimental Design

Construction of filtration systems on an unpaved road in a forested environment provided a metric for determining if the treatments were practical to implement on a large scale. Although construction of the sand filter and geotextile berm was moderately labor intensive, laboratory analysis of the geotextile filter fabric and sand filter indicate a marked sequestration benefit that may substantiate the higher cost of installation.

Two main failure mechanisms are posited for the Douglas fir biomass filtration system. The first, is the density of the biomass pack. Although much time was taken to densely pack the Douglas fir biomass product into sand bags, the end result still had high volumes of void space and high permeability. Given the rate of rainfall applied to the system, the berm was not able to slow runoff enough to allow sediments to settle out prior to entering the ditch. The second failure mechanism was directly observed during testing. The biomass filter bags became buoyant when runoff was high, allowing the water to flow along the channel liner (the bottom of the in-situ runoff collection flume), under the biomass bale, and directly into the ditch. Had the channel liner not been present, it is possible that the biomass bales could have been secured to the subgrade to prevent flotation. Additionally, the berms could be entirely buried in the road margin which may also prevent flotation. Both of these potential solutions are labor intensive and do not address the first failure mechanism. While it is possible that the Douglas fir biomass product could provide a filtration benefit in a different setting, the construction techniques used in this study prevented this from being a useful sediment sequestration treatment.

CONCLUSION

Of the two filtration treatments applied to an unpaved forest road, only one produced a quantified benefit of improved aggregate performance and sediment sequestration. The use of geotextile fabric, in combination with a filter sand berm and geogrid-reinforced subgrade provided the greatest benefit. The use of Douglas fir biomass bales did not provide a sediment sequestration benefit. Construction of the biomass berm may have led to its ineffectiveness but field observations indicated that the lack of adequate interlock between the berm and adjacent aggregate prevented it from being a viable road treatment.

Efficacy of both sediment filtration prototypes was hindered in field testing by the impermeable channel liner material. Follow up laboratory tests of idealized conditions showed an average reduction in effluent turbidity of 78 % when the Stayton filter sand was wrapped in non-woven geotextile. Flushing times under these conditions were shown to be less than 20 minutes.

Both turbidity and suspended solids concentration revealed periodicity and flushing patterns corresponding to the initiation and termination of truck traffic every 100 passes. Flushing was also seen in the permeameter filtration tests. This verifies established understanding that truck traffic is a driver of sediment generation. Minimal time to concentration of sediment transport off the road during a rainfall event mirrors the recovery rate of road effluent during non-traffic flushing of the roadway.

Geogrid reinforcement improved load distribution for both well-graded and poorly-graded aggregate varieties. Rutting depths were reduced for well-graded aggregate used with the geogrid but rutting depths were not reduced for poorly-graded aggregate using the geogrid. The data indicates the low contact area between aggregate particles of the poorly-graded aggregate reduced load distribution capabilities. Degradation of aggregate particles as a result of truck traffic began to fill voids in poorly-graded aggregate with a range of particle sizes. Degradation of well-graded aggregate produced mostly fine particles as a result of the limited void space available. These trends would be consistent with the hypothesis that the roadway is moving towards an ideal fines percentage which maximizes road bearing strength and minimizes runoff energy.

The application of geotextiles in this study on an unpaved forest road provide both sediment sequestration (under idealized conditions) and improved aggregate performance. Geotextile applications to filter runoff are moderately labor intensive and slow the speed of construction while geogrid placement is straightforward and less likely to slow the pace of road construction. It is practical to use a geotextile filtration system on segments of road that are prone to high sediment delivery given the sequestration benefits discovered in this study. Furthermore, use of geogrid on unpaved forest roads is practical for most areas assuming easy transportation of the material. Given the water quality benefits and reduced road maintenance, the geotextile treatment deserves both further investigation into use on a larger scale and is appropriate for small scale field application based on the positive results of this study.

REFERENCES CITED

Beschta, Robert L. 1978. "Long-term patterns of sediment production following road construction and logging in the Oregon Coast Range." *Water Resources Research* 14 (6): 1011-1016.

Bilby, Robert E., Kathleen Sullivan, and Stanley H. Duncan. 1989. "The Generation and Fate of Road-Surface Sediment in Forested Watersheds in Southwestern Washington." *Forest Science* 35 (2): 453-468.

Castelle, A. J., A. W. Johnson, and C. Conolly. 1994. "Wetland and Stream Buffer Size Requirements—A Review." *Journal of Environmental Quality* 23: 878-882.

Clegg, B. 1980. "An impact soil test as alternative to California bearing ratio." *Third Australia-New Zealand conference on Geomechanics: Wellington, May 12-16, 1980.* Wellington, N.Z.: Institution of Professional Engineers New Zealand. http://search.informit.com.au/documentSummary;dn=648478594123021;res=IELENG.

Foltz, R. B., and M. Truebe. 2003. "Locally Available Aggregate and Sediment Production." *Transportation Research Record* 185-193.

Giroud, J.P., and Jie Han. 2004. "Design Method for Geogrid-Reinforced Unpaved Roads. II. Calibration and Applications." *Journal of Geotechnical and Geoenvironmental Engineering* 130 (8): 787-797.

Goard, Deborah Lynn. 2003. "Characterizing the Spatial Distribution of Short Duration, High Intensity Raingall in the Central Oregon Coast Range." Master's Thesis, Oregon State University. Accessed April 10, 2015. http://hdl.handle.net/1957/9700.

Hardin, Bobby O. 1985. "Crushing of Soil Particles." *Journal of Geotechnical Engineering* 111 (10): 1177-1152.

Johnson, Michael G., and Robert L. Beschta. 1980. "Logging, Infiltration Capacity, and Surface Erodibility in Western Oregon." *Journal of Forestry* 78 (6): 334-337.

Lane, Patrick N. J., and Gary J. Sheridan. 2002. "Impact of an unsealed forest road stream crossing: water quality and sediment sources." *Hydrological Processes* 2599-2612. doi:10.1002/hyp.1050.

Langbein, W. B., and S. A. Schumm. 1958. "Yield of Sediment in Relation to Mean Annual Precipitation." *American Geophysical Union* 39 (6): 1076-1084.

Lekarp, F., U. Isacsson, and A. Dawson. 2000. "State of the Art. II: Permanent Strain Response of Unbound Aggregates." *Journal of Transportation Engineering* 126 (1): 76-83.

Leshchinsky, B., and H. I. Ling. 2013a. "Numerical modeling of behavior of railway ballasted structure with geocell confinement." *Geotextiles and Geomembranes* 36: 33-43.

Leshchinsky, Ben, and Hoe Ling. 2013b. "Effects of Geocell Confinement on Strength and Deformation Behavior of Gravel." *Journal of Geotechnical and Geoenvironmental Engineering* 139 (2): 340-352.

Lewis, Jack. 1996. "Turbidity-controlled suspended sediment sampling for runoff-event load estimation." *Water Resources Research* 32 (7): 2299-2310.

Luce, Charles H., and Thomas A. Black. 1999. "Sediment production from forest roads in western Oregon." *Water Resources Research* 35 (8): 2561-2570.

Madej, M. A. 2004. ""How Suspended Organic Sediment Affects Turbidity and Fish Feeding Behavior"." *USGS: Sound Waves Monthly Newsletter.* no. November 2004. http://soundwaves.usgs.gov/2004/11/research2.html.

2005. "McDonald-Dunn Forest Plan." Oregon State University: College Forests, June.

Megahan, W. F., and W. J. Kidd. 1972. "Effects of Logging and Loggin Roads on Erosion and Sediment Deposition from Steep Terrain." *Journal of Forestry* 70 (3): 136-141.

Miller, Rebecca H. 2014. "Influence of Log Truck Traffic and Road Hydrology on Sediment Yield in Western Oregon." Master's thesis, Oregon State University. Accessed February 5, 2015. http://hdl.handle.net/1957/49899.

NRCS. 2009. *Soil Survey of Benton County, Oregon.* United States Department of Agriculture.

OAR-340-041-0036. 2015. "Water Quality Standards: Beneficial Uses, Policies, and Criteria for Oregon." Oregon Department of Environmental Quality, April 15. http://arcweb.sos.state.or.us/pages/rules/oars_300/oar_340/340_041.html.

Reid, Leslie M., and Thomas Dunne. 1984. "Sediment Production From Forest Road Surfaces." *Water Resources Research* 1753-1761.

Sheridan, Gary J., Philip J. Noske, Robyn K. Whipp, and Namal Wijesinghe. 2006. "The effect of truck traffic and road water content on sediment delivery from unpaved forest roads." *Hydrological Processes* 20: 1683-1699.

Skaugset, Arne E., Christopher G. Surfleet, Matthew W. Meadows, and Joseph Amann. 2011. "Evaluation of Erosion Prediction Models for Forest Roads." *Transportation Research Record: Journal of the Transportation Research Board* 3-12.

Toman, E. M., and A. E. Skaugset. 2011. "Reducing Sediment Production from Forest Roads During Wet-Weather Hauling." *Transportation Research Record: Journal of the Transportation Research Board* 13-19.

Toman, Elizabeth M., Arne E. Skaugset, and Glen E. Murphy. 2006. "An Analysis of Opportunity Costs with Wet-Weather Timber Hauling." *International Journal of Forest Engineering* 17-23.

Toman, Elizabeth Meyeres. 2007. *Reducing sediment production from forest roads during wet-weather use.* ProQuest.

Wu, Cho-Sen, Yung-Shan Hong, Yun-Wei Yan, and Bow-Shung Chang. 2006. "Soil-nonwoven geotextile filtration behavior under contact with drainage materials." *Geotextiles and Geomembranes* 24 (1): 1-10.

APPENDICES

Appendix A: Dunn Forest road map and test track site location on 320 Rd.

Modified from McDonald-Dunn Forest Plan (2005).

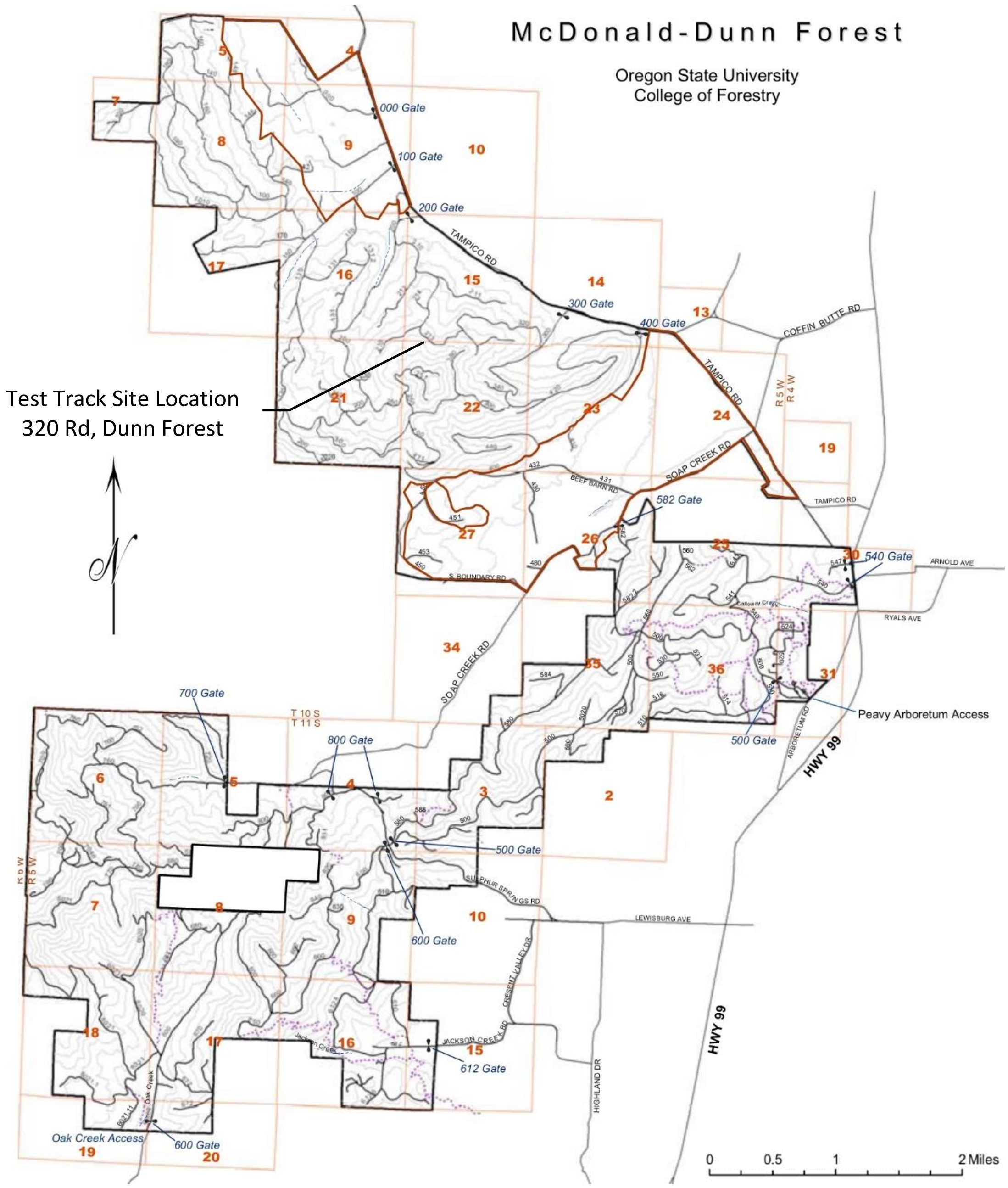

Appendix B: Properties of native subgrade material.

Clegg impact values - Inboard section of road

Section	Sample Number 1	2	3	4	Average
1	6.9	4.9	6.7	8.6	6.8
2	6.7	8.0	8.0	7.1	7.5
3	7.2	9.0	5.4	7.0	7.2
4	6.2	5.6	5.7	6.1	5.9
5	5.6	5.3	4.9	5.6	5.4
6	5.4	4.1	7.3	4.9	5.4

Vane shear - Undrained strength (kPa)

Section	Sample Number 1	2	3	4	5	Average
1	144	160	172	192	260	186
2	152	216	184	140	150	168
3	260	136	250	224	144	203
4	236	225	164	144	216	197
5	184	168	210	200	210	194
6	200	197	218	135	164	183

Water content of subgrade

Sample ID	Wet Mass w/ Core (g)	Mass of Core (g)	Wet Soil Mass (g)	Dry Soil Mass (g)	Water Content
1-1	328.25	147.54	180.71	131.08	0.38
1-2	375.80	143.93	231.87	173.44	0.34
1-3	379.69	149.29	230.40	166.25	0.39
2-1	374.34	152.51	221.83	159.79	0.39
2-2	379.60	151.92	227.68	160.22	0.42
3-1	393.03	146.60	246.43	176.07	0.40
3-2	388.39	147.43	240.96	177.70	0.36
4-1	400.53	147.43	253.10	192.69	0.31
4-2	380.14	147.44	232.70	185.77	0.25
5-1	402.53	147.37	255.16	201.36	0.27
5-2	408.39	147.26	261.13	201.25	0.30
6-1	402.77	147.52	255.25	196.69	0.30

Appendix C: Laboratory procedures for analysis of road runoff samples.

The following procedures are only those used for analysis of samples in this report. Please note that the dilution procedure for turbidity samples was modified for this project in consideration of the large number of dilutions required to process each sample.

LABORATORY PROCEDURES FOR DETERMINING SUSPENDED SEDIMENT CONCENTRATION

Oregon State University
Department of Forest Engineering

Revision Date:
11/25/13- Laura Bond
4/9/2013 – Alex Irving
2/18/2009 Mathew Quigley/Alex Irving
12/2008 Linda Ashkenas-includes acid-washing for chemistry samples
9/16/08 Chantal Goldberg

Table of Contents

Turbidity

Turbidity is the first step in processing a sample. The samples should be processed in approximately the same order in which they arrive at the lab. This limits the amount of evaporation from the bottles, reduces fading of the labels, and generally keeps the processing as parallel to the sampling as possible.

Materials

- Large Kimwipes
- Squeeze bottle filled with DI water
- Turbidimeter (Hach 2100P) with 3 Gelex secondary standards and at least 1 sample vial
- Waste bucket
- Macro balance able to handle load of one sample bottle filled with sediment and water
- Washed bottles with DI water for blanks

Procedure

1. Organize samples in numerical order. Since condensation forming on the vials can affect the turbidity reading of the sample, allowing them to warm on the tabletop will increase accuracy and efficiency.
2. Record bottle number, sample date, and add these samples to the appropriate spreadsheet.
3. Create blanks for the dump. (See Appendix: Creating Blanks)
4. Set up turbidimeter by running Gelex secondary standards to verify accuracy of calibration.
5. Shake ISCO sample bottle several times to re-suspend sediment in solution.
6. Pour an aliquot of sample into clean sample vial over the waste bucket
7. Clean sample vial with a large Kimwipe.
8. Wipe off remaining particles on outside surface and apply silicone with the black soft cloth and align vial in turbidimeter – diamond orientated towards the front aligned with the dash on unit.
9. Record turbidity on the SSC spreadsheet.
10. Pour contents of sample vial into the waste bucket and rinse sample vial 3 times with DI water using the squeeze bottles.
11. Does the turbidimeter read >1000? If so, see Turbidity Dilutions.
12. Record the turbidity value in the spreadsheet.
13. Repeat for all the bottles, including the blanks.
14. The blanks should have a turbidity below 0.15 NTU. If it doesn’t, clean the vial more carefully. If it still reads too high, check the DI water. If this water is not crystal clear, it is an indication that the filter may not be working correctly.
15. Once done with the bin, update the Sample Log sheet with date and initials indicating turbidity has been run.
16. Initial the turbidity box on both the bin label and the sample log indicating that

turbidity has been run.

Turbidity Dilutions

Turbidity Dilutions are done when the turbidity value is >1000. The turbidimeters we use do not read values that high. In order to get a turbidity estimate, the sample is diluted and the true turbidity is calculated.

Materials

- 5mL Pipette and tips
- Small bottle of deionized (DI) water (for diluting)
- Clean beaker for mixing the solution

Procedure

1. Thoroughly shake the sample.
2. Using the pipette, take ~~a known volume such as~~ *5ml and put it in the clean beaker*.
3. Add ~~a KNOWN amount of~~ *10 mL DI water to the sample*, ~~such as 10ml~~ (using the pipette).
4. Mix this solution and take a reading.
5. If the turbidity value is below 1000, record the value in the comments section and record how much sample and how much DI was used.
6. Calculate the turbidity. Example: If 5mL of sample and 10mL of DI produce a turbidity of 555 NTU:

$$(\text{Measured turbidity})\left(\frac{\text{Sample Volume} + \text{DI Volume}}{\text{Sample Volume}}\right) = \text{Sample}'\text{s turbidity}$$

$$(555\ \text{NTU})\left(\frac{5\ \text{mL} + 10\ \text{mL}}{5\ \text{mL}}\right) = 1665\ \text{NTU}$$

7. Type the calculated turbidity into the excel sheet.
8. If the calculated turbidity value is still above 1000 NTU, ~~dump out the current mix and make a new one. This time add more DI.~~ *Create another dilution using 10 mL of DI water and 5mL of the already diluted sample.*
9. Rinse out the pipette when you are done with it.

Weighing Sample Bottles

Weighing a bottle usually happens just after the turbidity of that bottle has been measured.

Materials

- Macro scale

- RSKey program

Procedure

1. **After** turbidities have been run, weigh each sample bottle on the macro scale.
2. Tare balance and make sure the balance is level by examining level bubble. If it is not in the black circle (which indicates balance), adjust the dials on balance legs/feet until bubble rests in that black circle.
3. Check to see the last time the balance calibration was completed. It should be done at least once a week. Check calibration if necessary on the calibration log sheet taped to the door of the cupboards.
4. Remove cap from sample bottle and weigh. Record weight in spreadsheet using the Print function on the scale and the RSKey program.
5. Repeat for all samples being processed.
6. Initial and date spreadsheet to indicate bottles weighed.
7. Initial ‘weights’ on bin label indicating that weights have been taken.

Filtering Normal Samples

This procedure is for samples that are **not** Trask Rush samples, which is most. If uncertain whether a Trask sample is a Trask Rush sample, check the description included in the Rush samples. If still not certain, do not filter and contact Alex to ask.

Materials

- Forceps
- Baking pans lined with aluminum foil
- Squeeze bottle filled with DI water
- Aluminum foil cover sheet
- Vacuum pump
- Filtrate carboy
- Vacuum filtration manifold with Buchner funnels
- Vacuum pressure hose/rubber stopper/copper tube assembly for filtrate carboy and vacuum line
- 1.5 µm glass fiber filter paper (Whatman 934-AH) sized to fit Buchner funnels – **Always handle glass fiber filter papers with forceps/tweezers**

Procedure

1. Retrieve sample bin from cooler and arrange samples in numerical order to minimize confusion.
2. Check the filtrate carboy. Do this before filtering and between each bin. Empty the carboy if there is filtrate in the carboy.
3. The vacuum pump connected to the filter manifold needs very little attention in the filtering process beyond turning it on and off. If something does seem to be wrong with it, check the pump manual (located T:\Groups\ASLab\Equipment\Vacuum Pump for filtering) and contact Alex. **Remember**: the top gets hot when it has been in use for a while.
4. Check the turbidities of the samples to be processed. Samples with large amount of

sediment can clog themselves on the regular filters. There are two ways to deal with this.

a. Method 1: If you know ahead of time that a regular sample is going to be a problem (high turbidity and/or a thick layer of sediment at the bottom of the bottle) you can use the large filter. For procedure on how to set up the large filter manifold, see Appendix: Large Filters. Once the manifold is set, use the same procedure for the rest of the process with the large filters.
b. Method 2: If you have already began to filter a sample and find that the sample filters very slowly, filter what you can on the first filter and filter the remainder on a second filter.

5. Take oven dry filters from the cabinet that have previously been numbered and weighed. Place the sample bottle under the funnel which will hold its filter.
6. Seat filters with numbered side **down** in the vacuum filter cups.
7. Record filter numbers in the excel sheet for the bottles which will be filtered
8. Wet filters with approximately 25 – 50 ml of DI water using the squeeze bottle. This will create a seal and prevent floating of the filter paper during sample filtration.
9. Turn on the vacuum making sure that at least two (2) lines of the manifold are open/on. Check for holes in filters - if there is a hole, the air will make a whistling sound. If so, replace filter with another number, and record new filter number on SSC spreadsheet.
10. Remove the lid from the bottle. If the bin has regular bottles, place the lid in the white bucket on the floor beside the filtration station.
11. Pour a small amount of sample into the funnel **slowly**, taking care that suction is continuously maintained.
12. Add any remaining sample to the appropriate filter (i.e. rinse the sample bottle with DI water and pass it through the filter.).
13. Rinse the filter cup sides with DI water to ensure all sediment has been removed from bottle and now resides on the filter.
14. When **all** the particles have been removed from the bottle, the bottle can be placed back in the bin to be washed.
15. Turn off the vacuum and carefully remove the filter with forceps. Place filters on foil lined baking pan. If the filter has large amounts of loose sediment present, place the filter in an aluminum dish inside the oven pan.
16. Clean funnels with DI water and large Kimwipes between samples and after use.
17. Record spills, errors, or notes in the comment column of the spreadsheet. It is important to record any observations or suspicions that may explain unusual results.
18. Once the baking pan is full cover the pan with a piece of foil.
19. Dry the filters in the ovens at 105^0C for 24 hours. This removes all the water from the sample. Each oven can hold 9 baking pans, 3 pans per shelf.
20. Indicate on oven log when the filters were placed in the oven and when they can come out.
21. Update the oven whiteboard to indicate where in the oven the pans were placed. Three pans can fit across a shelf in the oven so each third of the white space represents a baking pan. If two or three pans share a site and dump, their pans can be labeled together.

22. Once the bin is filtered, date and initial the “filtered” and “to be Washed” section on the bin label and place the bin on the washing shelf between the two offices.
23. Initial and date the sample log to indicate that filtering is done.
24. At the end of filtering the bin, unplug the filtrate carboy from the tubing by pulling out the black stopper on the top.
25. Dump out the filtrate carboy into the plants outside the door of the lab. **The filtrate carboy is glass, time consuming to replace, and lacks handles**. Because of this, it lives in a bucket with a handle. Please **leave it in that bucket** and be careful when dumping out the filtrate.

Weighing Filters

Materials

- Oven at 105º C
- Oven gloves
- Forceps/tweezers
- Baking pans and aluminum foil
- Analytical balance accurate to 0.0001 gram for weighing filters
- RSKey program
- Desiccator cabinet
- Plastic Petri dishes
- Plastic bags (possibly)

Procedure

1. After 24 hours, remove the baking pan from oven. **Always use the oven gloves to handle hot objects**. These are located in the drawer near Oven #1.
2. Place a third oven glove on the counter so the baking pan does not hurt the counter and set the baking pan on top of it.
3. Place the filters in desiccant cabinet to cool for at least 10 minutes before weighing. Do not remove filters from desiccant cabinet until you are ready to weigh them since they will absorb moisture from the air.
4. Tare analytical balance and make sure the balance is level by examining level bubble. If it is not in the black circle (which indicates balance), adjust dials on balance legs/feet until bubble rests in that black circle.
5. Check the calibration log posted on the cupboard doors to see the last time the balance calibration was checked. It should be done **once a week**. Check calibration if necessary.
6. Weigh each filter and record the weight on SSC spreadsheet using the RSKey program. Record initials on SSC spreadsheet indicating you were the one to weigh the filters.
7. If the filter is a **large** filter, place it in a sandwich bag. These are in the drawer under the oven whiteboard.
8. Once this has been repeated for all the filters in the dump, stack the filters in order from first on top to last on the bottom in stacks of less the 13 samples. If the dump had more, split the dump into 2 stacks.

9. Tape each stack together with the label tape.
10. Label the stack.
11. Place in the correct location box located next to Oven #2.

Washing Regular Bottles

Materials

- Sponge/Long-handled, bristled brush
- White bucket for DI water
- large Kimwipes
- Soap

Procedure

1. Bins to be washed are placed on shelves near the sink.
2. Fill the left side of the sink with soapy water. Use the liquid-nox solution kept in the squeeze bottle by the side of the sink. This is the wash.
3. Fill the right side of the sink with plain water from the tap. This is the first rinse.
4. Fill a white bucket with DI water from the DI carboy. This is the second rinse.
5. Empty the bottles from the bin onto a cart and place large Kimwipes on the bottom of the bin.
6. Place about 6 bottles in the wash and scrub them with the bristled brush. Fill the bottle with some of the wash water and shake the bottle to rinse all the sides. Do this 3 times per bottle then transfer the bottle to the first rinse.
7. In the first rinse, fill the bottle with some of the wash water and shake the bottle to rinse all the sides. Do this 3 times per bottle then transfer the bottle to the second rinse.
8. In the second rinse, fill the bottle with some of the wash water and shake the bottle to rinse all the sides. Do this 3 times per bottle then place the bottle top down on the Kimwipe in the bin.
9. Once the bin is full, place the bin on the table located near the micro scale to dry.
10. The white bucket on the floor beside the filter station is often filled with lids. Those are washed as well. The dirt and particles is scrubbed off of the lids in the wash, and then the lids go through both rinses.
11. For drying the lids, place two large Kimwipes covering a baking sheet. Place the lids on this sheet top up so they do not hold water.
12. Pans of lids are placed in the same place as the bins of clean bottles.

Weighing Empty Bottles

Materials

- Macro scale
- RSKey program
- Bag of clean lids that match the bottle type

Procedure

1. Once bottles have dried completely, weigh (without caps) on macro balance and record weights on SSC spreadsheet using the RSKey program.
2. Remove labels from bottles.
3. Cap the bottle with a clean lid. Clean lids are on the washing shelf in the white buckets.
4. Remove the large Kimwipes from the bottom of the bin and remove the bin tag. Place the empty bin in the pile by the clean full bins.
5. Put 24 clean bottles in a bin and stack the bin of clean bottles in the corner of the lab.
6. If there are extra dry lids on the drying table, they are placed in the bags in the white buckets on the wash shelves.

Appendix: Creating Blanks

Blanks are bottles of DI water which are processed identically as the rest of the samples.

Materials

- Clean bottle which matches the type in the bin from the bins of blanks below oven #2
- matte tape

Procedure

1. Using a clean ISCO bottle located under the cabinets in the bin marked blanks, create a “Blank” by filling with approximately 300mL of DI water from the large DI carboy by the sink.
2. Using the matte tape in the office supply drawer, label the blanks.
3. Blanks should be placed every 12 bottles apart in a dump at most. This means that in a dump of 24 bottles, there should be 2 bottles. 1 blank goes after 12 and one at the end of the dump. If the dump has only 12 or less bottles, only one blank is needed.

Appendix: Large Filters

Large filters are a solution to the time consuming process of filtering very thick samples. There are only large regular filters.

Materials

- Large Filters
- Large filter manifold. This is located on the counter behind the regular manifold

Procedure

1. Gather the large filters from the same shelf as the regular and Trask filters. They are marked large filters and are larger than regular filters.
2. Place the Large filter manifold on the filtration station in front of the regular manifold, making sure the tube connection is on the left
3. Disconnect the flask line from the flask and connect it to the manifold
4. Open the vacuum line to the flask.
5. Wipe out the vacuum filter cups, it’s probably been sitting on that counter for a while.
6. Follow the same filtration steps as the regular manifold with all the samples with too much sediment.

Appendix: Computation of Suspended Sediment Concentration

Equations for computation of suspended sediment concentration:

SSC (mg/L) = (Mass of sediment x 1000000)/ Actual volume of sample (ml)

Mass of sediment (g) = Mass of sediment and filter (g) – mass of oven-dried filter (g)

Calculated volume (g) = Mass of bottle and sample (g) - mass of bottle (g)

Actual mass of water in sample (ml) = (calculated volume (g) - mass of sediment (g)) x (1ml/g)

Mass of sediment/particle density (2.65 g) converted to ml = (mass of sediment (g) / 2.65 g) x (1 ml/g)

Actual volume of sample (ml) = Actual mass of water in sample (ml) + Mass of sediment converted to ml

Note:
Assumption: density of water is 1gm/ml therefore 1 gm of water has a volume of 1 ml

Assumption: Particle density = 1 cc of soil = 2.65 g

Adapted from:

Method 2540D in: Clesceri, L.S., A.E. Greenberg and A.D. Eaton, eds. 1998. Standard Methods for the Examination of Water and Wastewater. 20th ed. American Public Health Association, Washington, DC.

USFS Redwood Sciences Lab Sediment Lab Manual. Laboratory Procedures for Determining Suspended Sediment Concentration. 13p. Arcata, California. http://www.fs.fed.us/psw/topics/water/tts/manuals/sedlab_manual.doc

Appendix D: Aggregate separation bag gradation pre-testing.

Well-graded aggregate – mass passing screen size (g)

D (mm)	Screen	WG 1	WG 2	WG 3	WG 4	WG 5	WG 6	WG 7	WG 8	WG 9
> 50	d > 2"	21,291.0	23,083.0	23,659.5	20,650.5	23,299.0	18,574.5	21,630.5	18,923.5	23,677.5
50	2"	19,567.0	21,649.5	21,054.5	16,500.0	20,380.5	14,481.5	18,557.5	13,259.5	22,313.5
37.5	1½"	14,060.5	14,339.0	14,405.5	9,182.0	14,659.0	7,183.5	12,989.5	6,468.5	17,538.0
25	1"	11,152.0	10,995.0	10,162.0	5,278.0	10,397.0	3,336.5	8,234.5	3,151.0	13,022.0
12.5	½"	6,048.0	5,711.0	4,911.0	2,478.5	5,193.5	1,104.5	4,160.5	1,099.5	7,025.0
9.5	⅜"	4,911.0	4,675.5	3,878.5	1,988.0	4,167.0	799.0	3,396.0	771.5	5,795.5
6.3	¼"	1,858.5	2,547.0	2,317.0	1,113.5	2,391.0	461.0	1,987.5	386.5	3,345.0
	Totals	21,291.0	23,083.0	23,659.5	20,650.5	23,299.0	18,574.5	21,630.5	18,923.5	23,677.5

Poorly-graded aggregate – mass passing screen size (g)

D (mm)	Screen	PG 1	PG 2	PG 3	PG 4	PG 5	PG 6	PG 7	PG 8	PG 9
> 50	d > 2"	20,201.0	20,326.0	20,578.5	20,517.5	19,965.0	19,612.0	19,883.0	19,717.5	20,273.5
50	2"	20,201.0	20,326.0	20,578.5	20,517.5	19,965.0	19,612.0	19,883.0	19,717.5	20,273.5
37.5	1½"	20,127.5	20,167.0	20,578.5	20,517.5	19,818.5	19,612.0	19,883.0	19,426.0	20,191.5
25	1"	13,918.0	14,019.5	10,708.5	11,683.5	8,858.5	8,658.0	11,506.0	9,303.0	9,958.0
12.5	½"	275.0	328.5	131.0	240.5	123.0	149.5	183.5	87.0	101.0
9.5	⅜"	176.5	212.5	102.5	150.5	107.5	111.5	129.0	87.0	89.5
6.3	¼"	126.0	137.5	95.0	113.5	104.5	104.0	121.0	83.0	86.0
	Totals	20,201.0	20,326.0	20,578.5	20,517.5	19,965.0	19,612.0	19,883.0	19,717.5	20,273.5

Appendix E: Aggregate separation bag gradation post-testing.

Well-graded aggregate – mass passing screen size (g)

D (mm)	Screen	WG 1	WG 2	WG 3	WG 4	WG 5	WG 6	WG 7	WG 8	WG 9
> 50	d > 2"	19,671.5	22,426.9	23,169.8	20,400.1	22,020.4	18,630.9	21,090.4	19,040.8	20,090.0
50	2"	18,387.0	21,058.6	20,967.1	16,563.2	19,757.9	15,197.8	18,138.5	14,724.6	19,257.9
37.5	1½"	13,210.7	14,796.5	14,570.0	10,198.2	14,118.5	8,630.7	13,129.4	8,234.2	15,504.7
25	1"	10,525.4	11,246.4	10,679.0	6,084.9	9,976.9	4,497.8	8,937.5	4,429.2	11,453.1
12.5	½"	6,418.4	6,261.8	5,694.8	3,004.0	5,396.9	1,956.4	4,870.3	1,865.6	7,339.2
9.5	⅜"	5,588.3	5,204.9	4,581.7	2,470.6	4,320.4	1,542.5	3,929.7	1,411.6	6,323.7
6.3	¼"	3,803.6	3,233.1	2,719.4	1,589.4	2,553.3	958.6	2,414.9	798.9	4,260.4
4.75	No. 4	3,787.3	3,224.6	2,707.0	1,569.9	2,540.3	949.5	2,399.2	788.5	4,245.9
2	No. 10	2,689.7	2,878.7	1,807.7	1,154.8	1,744.2	735.8	1,697.2	538.9	3,061.0
0.425	No. 40	1,865.1	2,682.7	1,174.7	829.0	1,129.9	562.3	1,183.1	361.9	2,126.7
0.15	No. 100	1,500.9	2,542.4	937.2	687.2	898.2	474.7	974.1	285.5	1,652.5
0.075	No. 200	1,332.7	2,436.7	821.4	601.5	784.3	380.7	850.6	249.0	1,403.5
	Totals	19,671.5	22,426.9	23,169.8	20,400.1	22,020.4	18,630.9	21,090.4	19,040.8	20,090.0

Poorly-graded aggregate – mass passing screen size (g)

D (mm)	Screen	PG 1	PG 2	PG 3	PG 4	PG 5	PG 6	PG 7	PG 8	PG 9
> 50	d > 2"	19,869.7	20,154.7	18,608.9	20,480.4	19,997.4	19,269.3	19,856.3	18,925.7	20,972.5
50	2"	19,869.7	20,154.7	18,608.9	20,480.4	19,997.4	19,269.3	19,856.3	18,925.7	20,972.5
37.5	1½"	19,795.9	19,996.0	18,608.9	20,480.4	19,852.5	19,269.3	19,856.3	18,768.2	20,972.5
25	1"	14,887.3	14,919.3	10,608.6	14,314.5	10,688.4	10,194.1	12,799.7	10,327.0	12,940.5
12.5	½"	932.9	697.7	786.6	994.1	675.4	1,225.7	573.0	872.2	1,711.2
9.5	⅜"	746.9	491.9	716.2	755.7	574.0	1,125.6	448.8	797.4	1,572.0
6.3	¼"	532.4	326.8	631.6	531.8	419.1	974.7	335.9	603.7	1,368.3
4.75	No. 4	510.7	309.4	629.4	494.2	417.6	972.0	332.8	603.7	1,366.4
2	No. 10	410.1	244.1	550.5	397.0	335.8	892.0	268.9	459.7	1,224.7
0.425	No. 40	308.1	175.3	440.8	311.9	249.1	692.0	203.8	317.4	986.8
0.15	No. 100	248.4	120.5	349.0	259.1	188.1	592.0	162.1	243.6	742.2
0.075	No. 200	196.8	98.9	278.1	213.7	137.7	420.2	125.4	200.5	536.1
	Totals	19,869.7	20,154.7	18,608.9	20,480.4	19,997.4	19,269.3	19,856.3	18,925.7	20,972.5

Appendix F: Sample R code for pressure cell data reduction.

The following R code was used for each time grouping of pressure cell data (time when data loggers were turned on) in order to weed out data points that recorded when no truck traffic was occurring. This process also ensured that the record time stamps matched one another to provide a consistent time series among all six pressure cells.

```
rm(list=ls())

L1_05 <- read.table("/Users/Test/Google Drive/School/Thesis Research/Tables/L1
_Pressure_2014.07.01_1552_forR.txt",
                    header = T,
                    sep = "\t",
                    stringsAsFactors = F,
                    comment.char = "",
                    quote = "")

L2_05 <- read.table("/Users/Test/Google Drive/School/Thesis Research/Tables/L2
_Pressure_2014.07.01_1608_forR.txt",
                    header = T,
                    sep = "\t",
                    stringsAsFactors = F,
                    comment.char = "",
                    quote = "")

L1_05S <- read.table("/Users/Test/Google Drive/School/Thesis Research/Tables/L
1_Settings_2014.07.01_1552_forR.txt",
                    header = T,
                    sep = "\t",
                    stringsAsFactors = F,
                    comment.char = "",
                    quote = "")

L2_05S <- read.table("/Users/Test/Google Drive/School/Thesis Research/Tables/L
2_Settings_2014.07.01_1608_forR.txt",
                     header = T,
                     sep = "\t",
                     stringsAsFactors = F,
                     comment.char = "",
                     quote = "")

#L2_05S$Strain_2 <- -240.8663 # From previous record same day
print(L2_05S) # Make sure that new value is part of table

##   TIMESTAMP RN_B2 Strain_1  Strain_2  Strain_3
## 1   07:42.7   2984 175.3421 -240.8663 -403.0633

L1_05$Strain_1.1 <- abs(L1_05$Strain_1 - L1_05S$Strain_1)
L1_05$Strain_1.2 <- abs(L1_05$Strain_2 - L1_05S$Strain_2)
L1_05$Strain_1.3 <- abs(L1_05$Strain_3 - L1_05S$Strain_3)
```

```
L2_05$Strain_2.1 <- abs(L2_05$Strain_1 - L2_05S$Strain_1)
L2_05$Strain_2.2 <- abs(L2_05$Strain_2 - L2_05S$Strain_2)
L2_05$Strain_2.3 <- abs(L2_05$Strain_3 - L2_05S$Strain_3)

max(L1_05$Strain_1.1)

## [1] 202.8869

min(L1_05$Strain_1.1)

## [1] 0.0431

max(L1_05$Strain_1.2)

## [1] 94.0761

min(L1_05$Strain_1.2)

## [1] 0.0239

max(L1_05$Strain_1.3)

## [1] 202.8492

min(L1_05$Strain_1.3)

## [1] 0.0492

max(L2_05$Strain_2.1)

## [1] 176.4579

min(L2_05$Strain_2.1)

## [1] 0.0421

max(L2_05$Strain_2.2)

## [1] NaN

min(L2_05$Strain_2.2)

## [1] NaN

max(L2_05$Strain_2.3)

## [1] 760.5633

min(L2_05$Strain_2.3)

## [1] 0.0367

# Need to figure out what numbers in L2_05$Strain_2 are NAN
test <- is.na(L2_05$Strain_2)
L2_05_is_na <- L2_05[test, ]
print(min(L2_05_is_na$Time)) # 0.648356

## [1] 0.648356
```

```
print(max(L2_05_is_na$Time)) # 0.672025

## [1] 0.672025

# The incomplete lines of data fall within the testing interval


library(ggplot2)


L1_plot05 <- ggplot(L1_05) +
  geom_line(aes(x = Time, y = Strain_1.1, col="red")) +
  geom_line(aes(x = Time, y = Strain_1.2, col="blue")) +
  geom_line(aes(x = Time, y = Strain_1.3, col="green")) +
  scale_x_continuous(name = "Time Stamp",
                     breaks = seq(.4,1.0,.01)) +
  scale_y_continuous(name = "kPa", breaks = seq(0,400,40)) +
  ggtitle("Strain Data 05.1")
plot(L1_plot05)
```

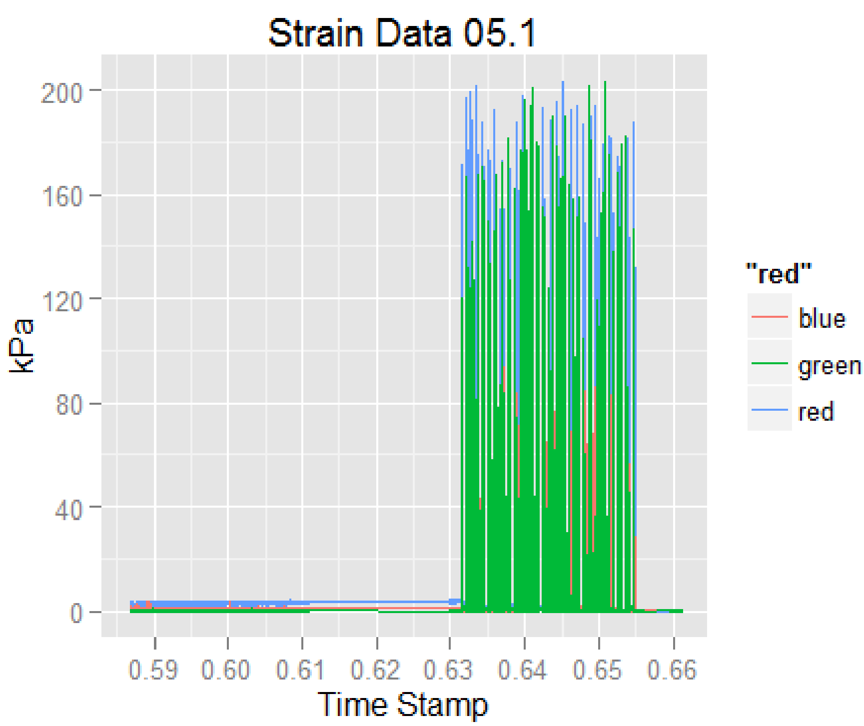


```
L2_plot05 <- ggplot(L2_05) +
  geom_line(aes(x = Time, y = Strain_2.1, col="black")) +
  geom_line(aes(x = Time, y = Strain_2.2, col="orange")) +
  geom_line(aes(x = Time, y = Strain_2.3, col="purple")) +
  scale_x_continuous(name = "Time Stamp",
                     breaks = seq(.4,1.0,.01)) +
  scale_y_continuous(name = "kPa", breaks = seq(0,400,40)) +
```

```
  ggtitle("Strain Data 05.2")
plot(L2_plot05)

## Warning: Removed 35946 rows containing missing values (geom_path).
```

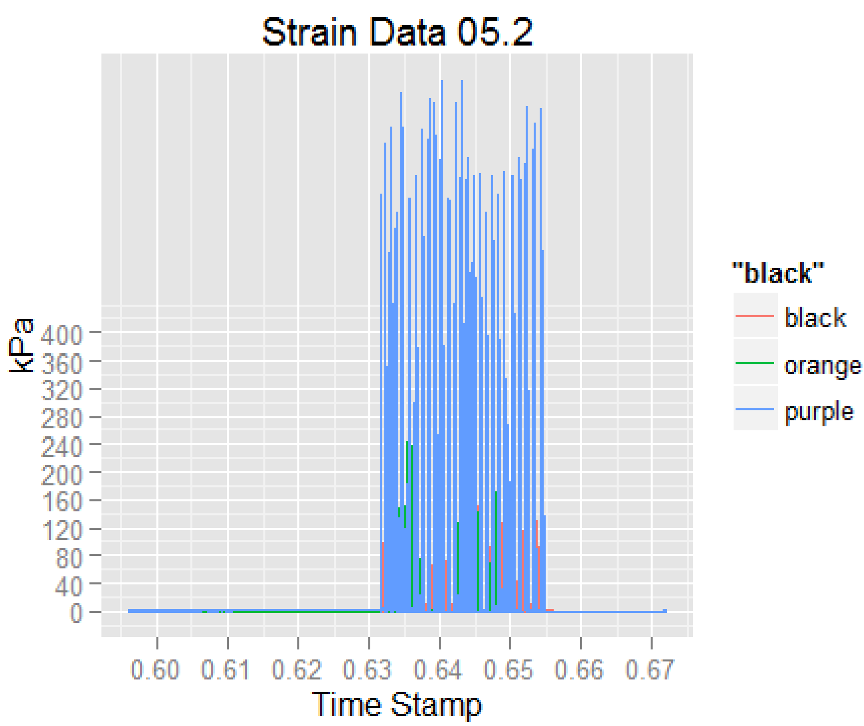


```
keep_rows1 <- 0.631 <= L1_05$Time & L1_05$Time <= 0.656
keep_rows2 <- 0.631 <= L2_05$Time & L2_05$Time <= 0.656
L1_05_w1 <- L1_05[keep_rows1, ]
L2_05_w1 <- L2_05[keep_rows2, ]

# Another iteration on plotting to verify correct points were removed

L1_plot05w <- ggplot(L1_05_w1) +
  geom_line(aes(x = Time, y = Strain_1.1, col="red")) +
  geom_line(aes(x = Time, y = Strain_1.2, col="blue")) +
  geom_line(aes(x = Time, y = Strain_1.3, col="green")) +
  scale_x_continuous(name = "Time Stamp",
                     breaks = seq(.63,.66,.002)) +
  scale_y_continuous(name = "kPa", breaks = seq(0,800,100)) +
  ggtitle("Strain Data 05.1")
plot(L1_plot05w)
```

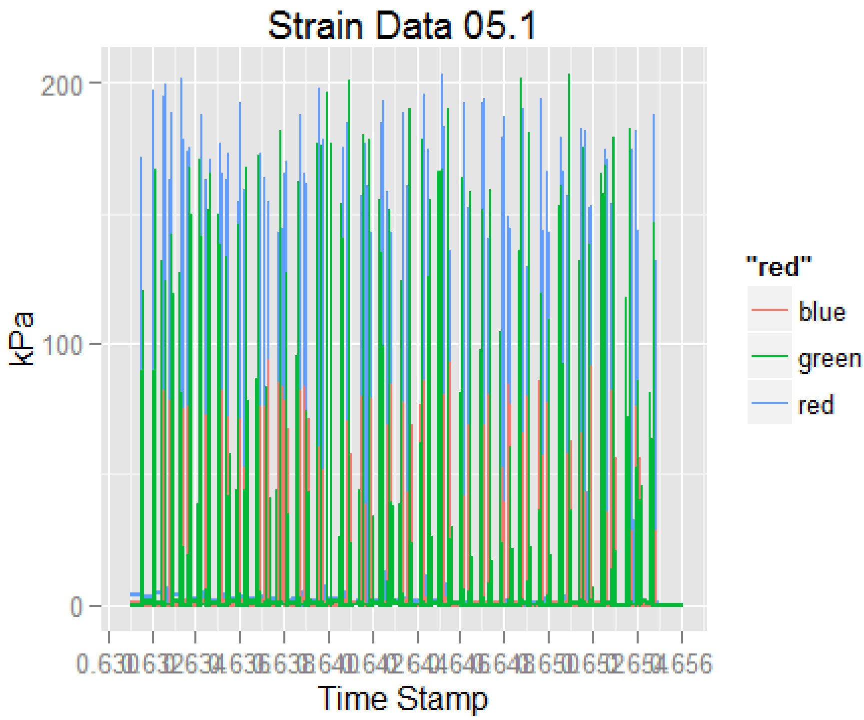


```
L2_plot05w <- ggplot(L2_05_w1) +
  geom_line(aes(x = Time, y = Strain_2.1, col="black")) +
  geom_line(aes(x = Time, y = Strain_2.2, col="orange")) +
  geom_line(aes(x = Time, y = Strain_2.3, col="purple")) +
  scale_x_continuous(name = "Time Stamp",
                     breaks = seq(.63,.66,.002)) +
  scale_y_continuous(name = "kPa", breaks = seq(0,800,100)) +
  ggtitle("Strain Data 05.2")
plot(L2_plot05w)

## Warning: Removed 32959 rows containing missing values (geom_path).
```

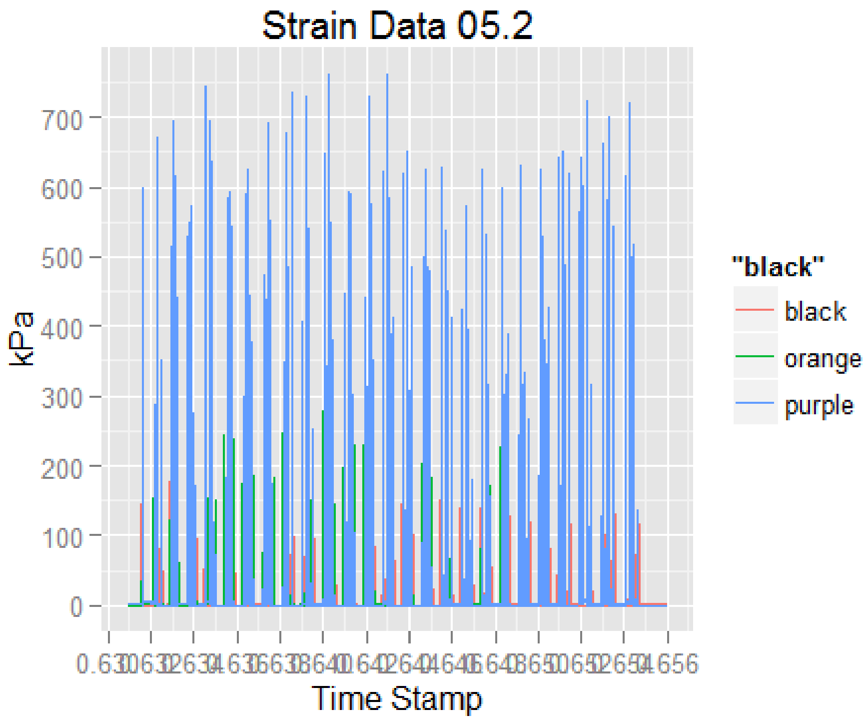


```
# New data frames with all six pressure cell data
L_05.1 <- data.frame(L1_05_w1$Strain_1.1, L1_05_w1$Strain_1.2, L1_05_w1$Strain
_1.3, check.rows = F)

L_05.2 <- data.frame(L2_05_w1$Strain_2.1, L2_05_w1$Strain_2.2, L2_05_w1$Strain
_2.3, check.rows = F)

L_05.1$Time_1 <- L1_05_w1$Time
L_05.2$Time_2 <- L2_05_w1$Time



write.table(L_05.1, file = "/Users/Test/Google Drive/School/Thesis Research/Ta
bles/L_05.1_0701_outR.txt", append = F, quote = T, sep = "\t", eol = "\n", na
= "NA", dec = ".", row.names = T, col.names = T, qmethod = c("escape", "double
"), fileEncoding = "")

write.table(L_05.2, file = "/Users/Test/Google Drive/School/Thesis Research/Ta
bles/L_05.2_0701_outR.txt", append = F, quote = T, sep = "\t", eol = "\n", na
= "NA", dec = ".", row.names = T, col.names = T, qmethod = c("escape", "double
"), fileEncoding = "")
```

Appendix G: Maximum subgrade stress at each pressure cell (kPa).

Pass	WGC	WGB	WGG	PGG	PGB	PGC
1	143	109	54	78	66	118
2	129	105	64	100	22	113
3	183	118	59	96	13	130
4	131	121	50	77	40	125
5	234	135	59	95	59	108
6	127	19	38	88	32	120
7	218	114	63	113	28	117
8	96	116	48	72	65	125
9	246	125	58	100	52	120
10	231	83	60	85	31	126
11	279	129	59	103	19	133
12	102	123	34	77	58	123
13	229	143	53	108	67	124
14	220	131	63	100	17	126
15	266	139	68	105	21	126
16	163	139	48	101	42	130
17	266	156	65	97	55	130
18	239	37	50	86	20	129
19	287	132	54	104	18	133
20	120	114	36	73	39	129
21	255	179	82	98	58	124
22	249	95	87	95	44	130
23	229	112	66	115	42	132
24	258	97	20	89	62	142
25	296	155	73	97	54	121
26	302	117	84	90	59	123
27	281	127	65	123	42	137
28	154	65	34	98	73	134
29	181	127	62	101	45	129
30	305	106	86	100	23	113
31	269	124	64	125	40	127
32	238	98	42	100	71	135
33	293	107	60	101	60	123
34	319	102	74	96	49	132
35	295	105	72	109	55	140
36	213	102	47	79	72	143

Pass	WGC	WGB	WGG	PGG	PGB	PGC
37	274	120	62	102	35	120
38	301	92	77	97	43	116
39	304	90	71	104	59	131
40	211	90	42	88	56	140
41	290	110	62	100	32	123
42	313	106	84	102	30	104
43	326	122	66	110	47	139
44	210	127	55	117	59	139
45	283	99	58	100	29	128
46	327	103	77	100	43	134
47	323	101	62	121	42	135
48	318	100	51	102	50	142
49	298	121	63	98	51	116
50	313	70	75	94	44	111
51	271	78	61	114	53	129
52	124	89	32	61	58	126
53	303	99	55	108	32	116
54	332	75	74	99	28	102
55	332	70	57	85	53	136
56	290	94	44	63	66	140
57	295	96	59	122	35	119
58	327	81	76	106	27	108
59	346	95	57	81	57	135
60	191	83	41	84	64	137
61	304	94	40	115	60	125
62	324	89	68	109	36	113
63	314	91	54	120	55	138
64	311	84	28	117	64	146
65	266	90	35	111	48	129
66	325	105	50	109	9	103
67	345	100	51	119	50	144
68	326	82	43	108	67	134
69	298	112	44	115	25	130
70	354	75	64	113	23	104
71	382	55	48	101	59	145
72	353	89	39	116	70	132
73	241	94	51	120	45	117
74	366	51	69	105	36	123
75	344	56	54	116	58	150

Pass	WGC	WGB	WGG	PGG	PGB	PGC
76	305	90	38	116	68	128
77	330	111	47	113	67	122
78	384	67	66	108	41	130
79	377	79	51	123	56	152
80	344	95	35	63	68	147
81	275	93	48	114	26	130
82	401	82	63	116	55	138
83	423	80	49	125	59	149
84	289	88	36	87	68	120
85	264	95	51	124	30	133
86	376	71	62	115	33	121
87	412	87	49	113	60	152
88	235	88	38	99	70	134
89	300	74	45	121	33	138
90	349	45	64	118	30	118
91	370	74	46	99	61	155
92	235	93	43	138	66	149
93	357	91	44	124	29	140
94	404	70	64	113	26	117
95	409	80	46	121	59	156
96	300	99	47	111	69	142
97	297	95	50	118	23	125
98	407	53	66	114	44	128
99	385	58	49	126	57	161
100	265	101	48	125	69	138
101	319	82	61	114	35	139
102	364	74	66	98	41	115
103	394	63	46	82	58	153
104	269	77	32	136	64	103
105	337	84	48	114	12	117
106	357	96	62	133	10	73
107	419	78	47	68	65	149
108	136	77	29	64	35	123
109	313	90	47	129	15	116
110	364	50	28	104	27	112
111	386	69	41	88	63	154
112	187	57	35	66	58	122
113	333	85	52	116	30	124
114	422	77	54	114	25	106

Pass	WGC	WGB	WGG	PGG	PGB	PGC
115	400	82	46	81	60	106
116	171	72	34	90	69	153
117	329	88	57	118	48	147
118	205	39	47	80	55	122
119	7	9	37	43	61	119
120	126	81	35	72	64	129
121	334	90	42	135	20	119
122	118	44	63	114	46	104
123	21	20	46	75	64	88
124	55	79	32	62	77	158
125	284	98	38	142	21	121
126	55	9	21	63	58	111
127	18	36	44	74	66	80
128	12	89	33	85	63	139
129	303	97	64	135	30	137
130	314	74	61	95	56	121
131	226	35	41	93	73	127
132	133	89	33	68	63	145
133	349	103	54	140	24	110
134	369	50	54	114	31	114
135	302	32	40	103	79	86
136	20	47	36	66	68	158
137	358	106	49	151	41	140
138	125	12	44	96	36	129
139	58	9	33	83	74	151
140	121	98	34	97	87	140
141	338	116	54	153	13	117
142	78	14	51	101	26	118
143	31	5	33	94	68	77
144	19	100	35	84	74	159
145	391	118	73	137	28	144
146	294	74	70	104	40	111
147	225	26	49	71	67	74
148	15	25	37	106	86	139
149	373	127	57	138	34	141
150	173	6	14	66	58	139
151	110	7	22	51	65	48
152	127	74	39	97	86	141
153	366	120	79	137	30	131

Pass	WGC	WGB	WGG	PGG	PGB	PGC
154	425	149	60	120	58	141
155	501	105	57	127	64	143
156	237	111	31	79	66	154
157	395	152	38	147	32	144
158	493	104	54	136	11	109
159	482	113	55	144	66	158
160	316	112	35	91	67	164
161	368	156	65	138	28	142
162	474	134	60	125	13	97
163	415	87	54	146	42	160
164	136	80	39	121	61	156
165	391	165	71	158	21	145
166	498	149	57	135	17	109
167	453	99	59	141	61	162
168	165	14	21	62	76	160
169	472	143	71	146	26	152
170	465	84	63	104	44	139
171	390	48	55	144	67	156
172	225	88	49	105	79	170
173	422	147	74	150	22	145
174	506	107	75	102	47	144
175	459	55	58	149	70	159
176	355	96	40	113	63	52
177	293	47	46	95	55	105
178	469	113	72	115	47	146
179	394	109	61	143	68	157
180	112	77	38	130	63	161
181	444	135	77	122	40	143
182	515	109	73	123	45	143
183	438	71	59	144	46	164
184	310	77	39	93	60	165
185	343	81	82	117	42	148
186	498	128	63	126	56	134
187	507	62	63	147	55	157
188	194	72	30	98	69	172
189	468	149	67	147	33	152
190	438	82	79	103	58	132
191	340	55	62	130	66	165
192	208	96	34	142	61	178

Pass	WGC	WGB	WGG	PGG	PGB	PGC
193	399	108	79	140	26	149
194	187	53	69	95	61	140
195	202	68	59	140	66	169
196	441	102	52	127	54	177
197	324	116	80	137	26	120
198	446	106	78	132	30	126
199	390	59	59	106	72	157
200	500	120	63	151	61	175
201	317	115	96	111	59	142
202	232	87	84	116	47	148
203	239	55	63	135	47	159
204	397	106	61	154	60	171
205	291	90	85	149	33	146
206	469	88	59	64	63	139
207	328	59	59	124	66	167
208	470	147	67	119	44	171
209	422	156	80	162	24	144
210	387	100	61	78	63	131
211	313	62	63	126	63	173
212	345	125	59	136	61	179
213	373	136	90	173	19	136
214	255	70	58	92	65	131
215	147	57	62	101	69	170
216	283	109	64	119	60	176
217	474	167	77	128	31	141
218	570	138	82	101	63	108
219	511	60	64	129	71	148
220	321	146	62	96	56	174
221	415	123	76	126	22	120
222	367	22	19	42	67	145
223	308	58	64	124	67	174
224	212	122	40	92	50	179
225	351	68	72	124	26	133
226	379	42	32	59	67	125
227	4	3	2	67	70	164
228	4	3	40	112	50	158
229	341	93	74	92	27	144
230	373	30	37	82	63	136
231	297	71	58	115	63	168

Pass	WGC	WGB	WGG	PGG	PGB	PGC
232	352	100	37	113	49	156
233	523	193	73	113	34	138
234	591	104	66	75	65	137
235	517	107	69	127	70	165
236	409	71	37	113	44	149
237	561	152	77	116	34	133
238	510	70	34	58	62	141
239	445	52	45	89	70	164
240	287	92	37	87	48	154
241	462	161	77	111	38	136
242	484	122	58	81	65	130
243	445	50	54	83	71	152
244	473	106	36	85	43	170
245	436	155	71	135	21	131
246	475	128	65	98	58	132
247	418	42	62	92	70	145
248	359	94	49	164	50	160
249	434	169	86	134	27	136
250	513	124	80	99	37	130
251	462	72	62	102	60	169
252	223	103	46	169	40	177
253	463	77	67	98	34	140
254	449	44	36	70	43	138
255	387	61	49	81	58	166
256	289	89	41	118	42	178
257	551	141	83	119	41	138
258	440	75	40	43	54	118
259	368	54	61	94	68	165
260	297	110	41	141	48	179
261	513	141	89	137	39	143
262	294	51	38	50	61	114
263	253	29	58	76	73	165
264	385	76	39	93	46	182
265	511	153	84	141	26	140
266	534	135	73	109	65	139
267	459	104	80	136	58	163
268	381	116	40	128	66	181
269	544	171	83	145	23	120
270	374	55	33	64	66	139

Pass	WGC	WGB	WGG	PGG	PGB	PGC
271	374	91	72	142	63	174
272	307	105	42	135	50	180
273	586	148	57	151	22	119
274	550	132	68	120	67	140
275	427	25	65	125	69	170
276	153	125	49	128	61	184
277	504	159	69	167	16	112
278	547	158	85	112	67	138
279	533	149	79	143	65	172
280	222	88	45	125	46	158
281	583	177	75	161	20	124
282	515	147	59	145	35	137
283	558	77	77	130	63	174
284	264	85	52	60	38	159
285	574	173	97	124	31	131
286	542	111	66	87	65	128
287	505	115	82	145	56	176
288	175	102	47	142	49	159
289	522	173	72	151	53	139
290	540	134	77	119	62	138
291	488	119	84	149	66	173
292	411	86	54	139	53	160
293	518	167	86	136	60	133
294	392	82	81	72	44	107
295	371	61	84	132	68	161
296	182	74	52	115	65	178
297	519	170	99	143	29	138
298	513	68	59	86	67	124
299	497	102	85	132	66	173
300	161	93	46	89	44	139
301	285	70	91	108	56	112
302	343	35	35	35	63	111
303	340	24	33	130	60	136
304	415	106	79	135	50	114
305	441	57	62	84	74	129
306	456	24	17	14	52	35
307	389	25	43	63	67	87
308	472	107	89	155	67	141
309	398	94	87	87	71	114

Pass	WGC	WGB	WGG	PGG	PGB	PGC
310	555	82	27	17	53	58
311	465	60	43	50	72	93
312	533	127	89	98	77	98
313	352	80	77	87	79	121
314	571	108	87	26	55	47
315	479	104	91	138	61	135
316	494	101	94	126	69	123
317	431	109	93	102	73	136
318	498	61	36	58	78	140
319	466	84	62	92	53	143
320	585	93	81	103	91	117
321	292	31	83	128	86	124
322	33	11	41	53	61	64
323	33	24	69	173	39	158
324	403	75	98	159	61	152
325	359	38	57	92	85	131
326	370	26	27	24	67	113
327	380	17	48	51	75	131
328	529	122	104	153	70	136
329	543	135	66	74	85	133
330	407	27	75	11	39	6
331	410	27	94	94	73	105
332	597	148	99	131	84	115
333	533	118	101	91	82	126
334	559	32	25	30	90	127
335	572	69	80	113	74	167
336	628	139	104	140	76	127
337	597	164	118	115	85	135
338	573	110	56	27	65	32
339	572	59	59	76	81	148
340	578	126	109	157	57	123
341	517	135	71	74	72	130
342	385	151	104	76	85	125
343	506	107	87	86	75	111
344	590	132	116	155	70	125
345	324	62	106	111	68	121
346	541	115	99	53	66	98
347	468	101	98	156	65	157
348	508	135	89	146	79	116

Pass	WGC	WGB	WGG	PGG	PGB	PGC
349	469	190	116	120	82	132
350	540	64	59	50	91	118
351	473	69	78	88	68	126
352	541	154	95	132	77	170
353	597	171	80	91	86	144
354	537	157	98	69	69	101
355	471	17	53	50	79	79
356	163	181	92	150	86	93
357	504	155	98	93	70	111
358	524	77	58	44	96	135
359	329	115	78	85	70	127
360	489	154	94	164	75	114
361	451	156	88	57	81	133
362	526	161	86	57	70	56
363	445	96	89	167	66	153
364	332	124	90	124	70	121
365	495	197	105	99	85	139
366	546	74	53	58	77	83
367	427	88	66	92	59	146
368	413	132	90	149	74	129
369	389	90	86	83	67	74
370	526	190	89	37	92	142
371	375	115	96	146	74	180
372	468	103	83	166	61	123
373	331	118	91	113	82	142
374	422	43	72	77	91	125
375	276	111	96	179	79	186
376	479	162	92	179	89	133
377	447	187	108	116	87	161
378	376	31	44	37	95	139
379	310	72	58	94	74	182
380	483	176	95	177	69	104
381	491	186	104	111	72	115
382	368	16	34	37	90	137
383	320	109	89	94	88	143
384	537	191	92	160	86	140
385	415	105	72	79	84	149
386	387	32	80	76	81	114
387	352	28	65	100	81	93

Pass	WGC	WGB	WGG	PGG	PGB	PGC
388	608	190	95	168	86	109
389	373	99	106	114	80	110
390	591	112	61	72	66	122
391	460	75	97	112	79	132
392	549	200	96	130	84	81
393	362	74	105	90	80	132
394	533	149	99	94	81	165
395	412	99	99	131	75	137
396	552	214	97	151	70	105
397	522	147	107	106	86	141
398	563	24	73	82	92	144
399	380	31	100	150	79	175
400	605	202	101	165	86	165
401	352	97	93	62	79	118
402	566	87	64	70	73	101
403	391	37	61	85	79	119
404	548	195	100	166	79	117
405	432	162	116	85	84	121
406	549	82	49	47	79	125
407	428	49	65	89	79	101
408	572	210	116	163	83	171
409	641	193	118	97	68	148
410	536	88	60	84	70	145
411	414	56	80	108	86	144
412	679	160	106	158	90	147
413	377	141	106	120	84	151
414	414	59	72	95	94	129
415	390	74	89	111	81	153
416	562	193	98	162	88	152
417	392	113	108	127	74	155
418	458	44	73	91	52	183
419	338	33	66	81	82	119
420	231	52	111	155	85	146
421	478	197	128	146	85	150
422	498	116	88	109	76	177
423	398	46	86	147	73	158
424	384	156	111	173	89	146
425	442	123	86	108	66	166
426	467	34	47	85	81	175

Pass	WGC	WGB	WGG	PGG	PGB	PGC
427	349	31	76	125	88	121
428	659	187	115	175	76	136
429	609	192	140	128	77	163
430	618	44	51	49	75	126
431	371	20	40	138	86	189
432	681	196	85	171	78	170
433	389	127	127	136	76	163
434	567	28	67	93	86	125
435	357	40	82	151	80	169
436	806	176	77	161	83	167
437	562	146	63	100	82	151
438	422	51	63	72	72	107
439	421	32	48	87	86	142
440	588	213	103	153	79	153
441	629	180	81	99	85	156
442	442	20	10	25	94	160
443	431	39	69	75	81	195
444	356	82	99	163	70	180
445	630	278	76	120	84	157
446	631	97	41	38	94	132
447	462	14	48	60	87	126
448	256	72	104	165	73	158
449	662	279	101	92	84	127
450	624	105	41	90	99	154
451	518	62	76	107	83	187
452	221	85	110	181	74	147
453	642	251	81	93	67	190
454	662	128	97	62	79	142
455	451	23	78	117	84	152
456	410	120	104	181	49	196
457	570	211	130	120	84	159
458	668	83	51	70	68	173
459	477	41	81	120	72	191
460	603	198	105	183	42	183
461	564	217	139	153	86	144
462	660	106	37	35	66	183
463	365	18	58	49	78	134
464	143	209	112	181	46	173
465	536	214	155	158	84	157

Pass	WGC	WGB	WGG	PGG	PGB	PGC
466	649	124	34	46	90	156
467	505	49	72	77	78	125
468	578	140	96	189	34	180
469	468	225	138	135	74	111
470	615	195	56	39	81	143
471	472	17	62	90	79	125
472	154	152	116	177	76	188
473	394	209	165	178	66	177
474	690	72	54	104	78	166
475	470	38	53	91	76	124
476	647	180	103	155	84	196
477	686	248	120	125	89	166
478	655	135	39	41	92	153
479	442	58	61	61	84	133
480	186	105	70	178	63	178
481	85	112	159	137	74	170
482	685	54	53	52	65	70
483	467	44	72	86	84	132
484	365	51	97	193	72	165
485	91	181	138	118	67	175
486	702	24	35	40	87	124
487	505	42	80	127	83	165
488	120	114	75	159	75	159
489	313	131	153	132	83	166
490	651	194	45	35	86	148
491	520	67	61	41	68	132
492	412	151	46	153	88	165
493	722	155	124	150	80	178
494	673	39	32	28	91	175
495	326	16	38	40	80	139
496	243	56	66	166	55	167
497	417	173	143	187	81	153
498	436	23	43	27	86	167
499	339	119	84	138	81	176
500	360	49	100	161	71	168
501	598	214	145	120	83	171
502	287	185	139	167	48	197
503	672	204	80	132	82	195
504	352	106	76	124	48	199

Pass	WGC	WGB	WGG	PGG	PGB	PGC
505	515	244	176	142	78	163
506	694	168	58	120	58	188
507	615	149	60	127	75	202
508	440	60	53	82	75	178
509	548	249	158	168	76	174
510	572	18	43	150	61	175
511	275	11	35	39	70	171
512	172	148	95	171	82	187
513	744	238	165	151	73	163
514	695	235	147	165	53	171
515	637	148	92	150	69	177
516	117	151	87	138	82	165
517	182	243	148	133	80	163
518	584	88	32	58	72	173
519	593	15	34	44	80	154
520	542	238	91	146	71	193
521	298	224	159	167	52	159
522	626	192	89	78	71	163
523	443	26	71	86	84	154
524	377	184	90	172	76	173
525	474	76	40	84	76	164
526	692	123	45	34	94	154
527	551	11	33	44	85	143
528	174	183	100	182	85	159
529	350	247	122	127	78	165
530	678	47	29	34	87	170
531	486	20	73	95	77	130
532	734	231	97	162	82	188
533	407	121	52	75	84	165
534	730	186	69	43	69	161
535	540	149	109	176	60	198
536	252	181	95	176	52	178
537	648	278	148	196	67	170
538	760	223	142	177	86	150
539	550	62	47	26	79	152
540	380	145	89	153	82	175
541	448	238	125	201	70	184
542	592	25	26	24	69	104
543	590	158	38	44	80	157

Pass	WGC	WGB	WGG	PGG	PGB	PGC
544	301	230	114	180	38	177
545	443	247	150	178	85	160
546	730	85	36	34	79	142
547	576	27	65	155	79	184
548	352	126	85	135	68	193
549	621	316	135	152	69	158
550	761	166	37	40	84	143
551	585	18	30	39	83	50
552	412	212	85	124	77	188
553	619	309	146	190	43	160
554	651	21	29	24	87	158
555	407	21	31	62	76	138
556	484	209	102	179	86	195
557	500	202	118	155	71	174
558	624	18	28	26	86	150
559	486	154	81	166	57	203
560	478	183	105	167	80	183
561	629	327	152	190	82	175
562	537	16	24	30	93	135
563	449	67	33	81	79	140
564	414	179	116	163	41	192
565	425	285	138	158	69	152
566	573	16	24	19	85	149
567	396	28	37	98	79	193
568	178	69	93	152	69	194
569	625	318	139	159	81	140
570	532	15	17	17	63	140
571	315	24	30	105	53	179
572	157	170	55	24	39	187
573	599	225	54	61	84	149
574	302	7	23	22	76	144
575	330	0	68	136	48	192
576	388	0	126	202	66	190
577	630	0	159	181	80	130
578	318	0	13	23	85	159
579	333	0	12	36	86	194
580	266	0	119	119	58	143
581	624	0	52	109	78	166
582	528	0	12	19	90	142

Pass	WGC	WGB	WGG	PGG	PGB	PGC
583	381	0	49	153	66	179
584	427	0	81	161	66	166
585	643	0	159	203	58	157
586	651	0	22	37	62	155
587	489	0	20	132	66	183
588	620	0	117	175	50	181
589	642	0	109	138	83	152
590	603	0	1	7	91	153
591	722	0	55	165	51	174
592	315	0	122	168	49	171
593	664	0	115	179	82	153
594	581	0	103	20	58	139
595	701	0	65	118	73	173
596	542	0	130	182	46	175
597	618	0	93	86	76	182
598	720	0	132	45	56	144
599	516	0	73	81	81	187
600	137	0	115	146	37	132

Appendix H: Full pressure cell time series for all test sections.